TÄHT7039: Radio astronomy and interferometry

Kaj Wiik & Silja Pohjolainen

Tuorla Observatory

Spring 2015

Based partly on 'Essential radio astronomy' from http://www.cv.nrao.edu/course/astr534/Interferometers2.html and http://www.cv.nrao.edu/course/astr534/Interferometers2.html by J. J. Condon and S. M. Ransom.

Outline

Recap: Non-plane case, solution

$$V_\nu(u,v,w) = \iint \frac{I_\nu(l,m)}{\sqrt{1-l^2-m^2}} e^{-i2\pi(ul+vm+wn)} \,\mathrm{d}l\,\mathrm{d}m \qquad (1)$$

General form is not 3D FT, using small angle approximation we get:

$$V_\nu(u,v,w) = \iint \frac{I_\nu(l,m)}{\sqrt{1-l^2-m^2}} e^{-i2\pi(ul+vm+w\theta^2/2)} \,\mathrm{d}l\,\mathrm{d}m \qquad (2)$$

If $w\theta^2 \ll 1$ or $\theta_{max} \lesssim \sqrt{\theta_{synth}}$, it can be neglected. E.g. for a 0.1 milliarcsecond synthesized beam the limit would be about 144 milliarcseconds. Then further

$$V'_\nu(u,v) = \iint \frac{I_\nu(l,m)}{\sqrt{1-l^2-m^2}} e^{-i2\pi(ul+vm)} \,\mathrm{d}l\,\mathrm{d}m, \qquad (3)$$

which is again a 2D FT, yippee!

Recap: Sensitivity I

Antenna response:

$$K = \frac{\eta_a A}{2k} \cdot 10^{-26} = \frac{A_{eff}}{2k} \cdot 10^{-26} = \frac{T_a}{S} \left[\frac{\mathrm{K}}{\mathrm{Jy}}\right] = \mathrm{DPFU} \quad (4)$$

System response **SEFD**: what amount of source flux increases the system noise as much as the noise of the receiving equipment when $T_a = 0$:

$$\mathrm{SEFD} = \frac{T_{sys}}{\mathrm{DPFU}} = \frac{2kT_{sys}}{A_{eff}} \cdot 10^{26} \quad [\mathrm{Jy}] \quad (5)$$

Recap: Sensitivity II

Baseline sensitivity for antennas i and j (η_s = system efficiency):

$$\Delta S_{ij} = \frac{1}{\eta_s}\sqrt{\frac{\mathrm{SEFD}_i \cdot \mathrm{SEFD}_j}{2\Delta\nu\tau_{int}}} \quad [\mathrm{Jy}] \tag{6}$$

Image sensitivity I_m is standard deviation of mean of L samples (baselines),

$$\Delta I_m = \frac{1}{\eta_s}\sqrt{\frac{\mathrm{SEFD}_i \cdot \mathrm{SEFD}_j}{N(N-1)\Delta\nu\tau_{int}}} \quad [\mathrm{Jy/beam}] \tag{7}$$

Recap: Amplitude calibration: $\rho_{ij} \Rightarrow S_{ij}$

Raw correlator constant ρ_{ij} ($\propto V_{ij}$) must be calibrated to get **correlated flux densities**:

$$S_{ij}^{c} = \rho_{ij} \frac{b}{\eta_s} \sqrt{\frac{T_{sys}^{i} \, T_{sys}^{j}}{\mathrm{SEFD}_i \, \mathrm{SEFD}_j \, e^{-\tau_i} \, e^{-\tau_j}}}, \tag{8}$$

where

- ρ_{ij} = raw visibility
- b = correlator scaling factor
- η_s = system efficiency (digitization losses etc.)
- T_{sys}^{n} = system temperature at antenna n
- SEFD_n = system effective flux density at antenna n, incl. antenna gain vs. elevation
- $e^{-\tau_n}$ = atmospheric absorption at antenna n

Recap: Atmospheric opacity

T_{sys} plotted as a function of airmass ($T_{sys} \simeq T_R + T_0 \tau_0 \sec z$):

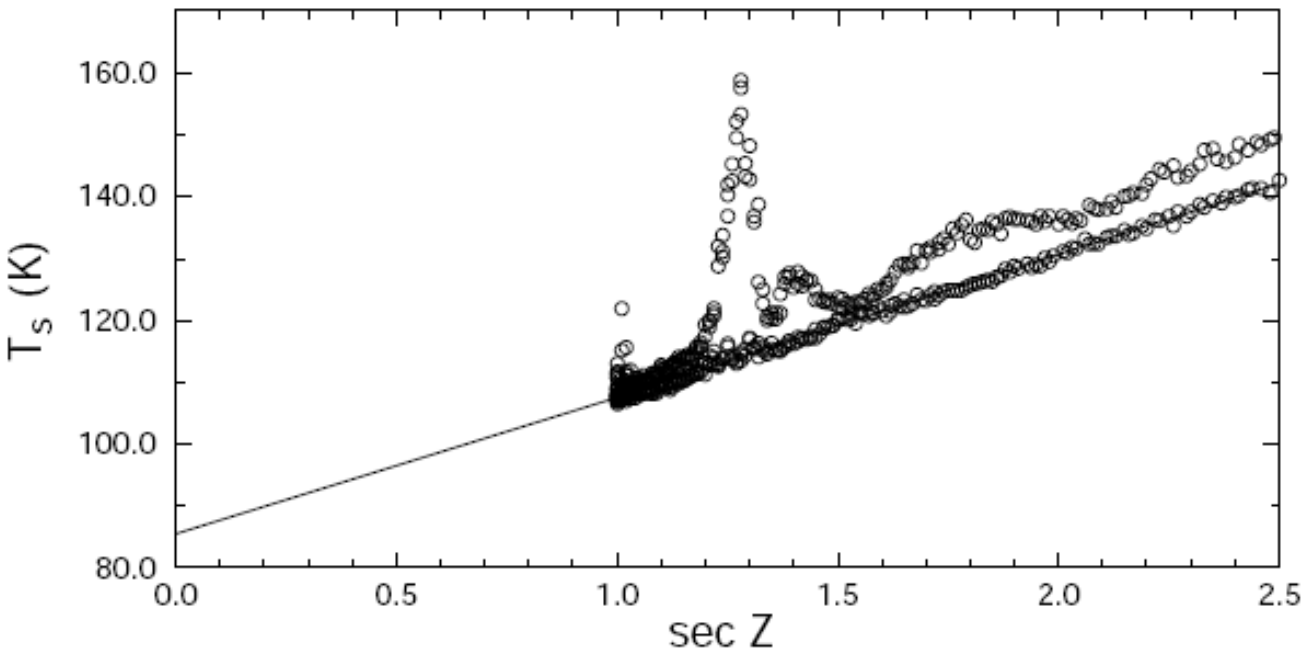

Zenith opacity τ_0 is the slope of the linear fit (times T_0) and $T_R = T_{sys}(\text{airmass} = 0)$

Figure from VLBA-book

Atmospheric opacity correction

- Corrections for absorption by the atmosphere
- Can estimate using T_s - T_r - T_{spill}

Example from VLBA single dish pointing data

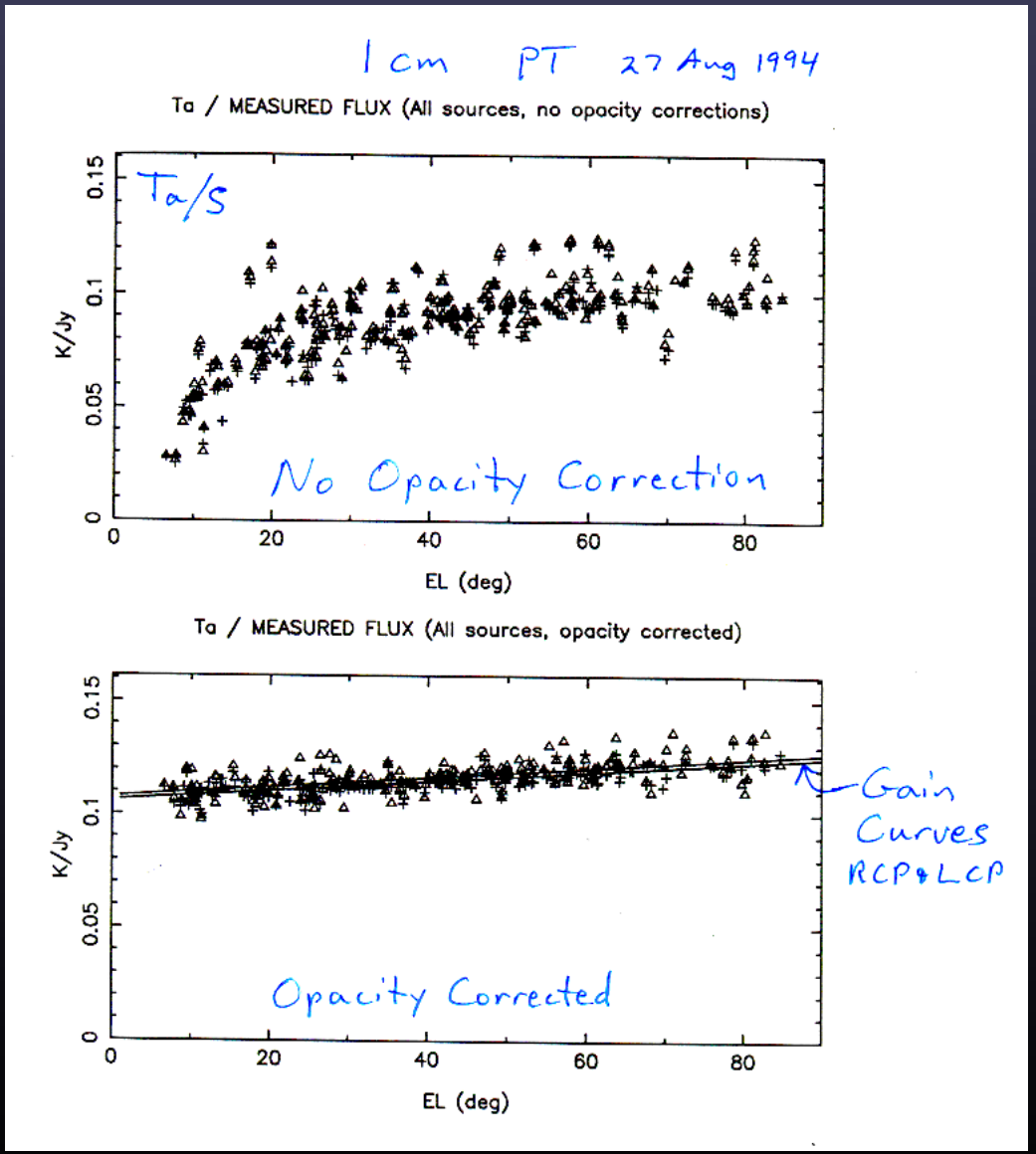

From: Ylva Pihlström, Craig Walker, Tenth Synthesis Imaging Summer School, UNM 2006.

Residual rate and delay

- Interferometer phase $\phi_{t,\nu} = 2\pi\nu\tau_t$
- Slope in frequency is “delay”
  - Fluctuations worse at low frequency because of ionosphere
  - Troposphere affects all frequencies equally ("nondispersive")
- Slope in time is “fringe rate”
  - Usually from imperfect troposphere or ionosphere model

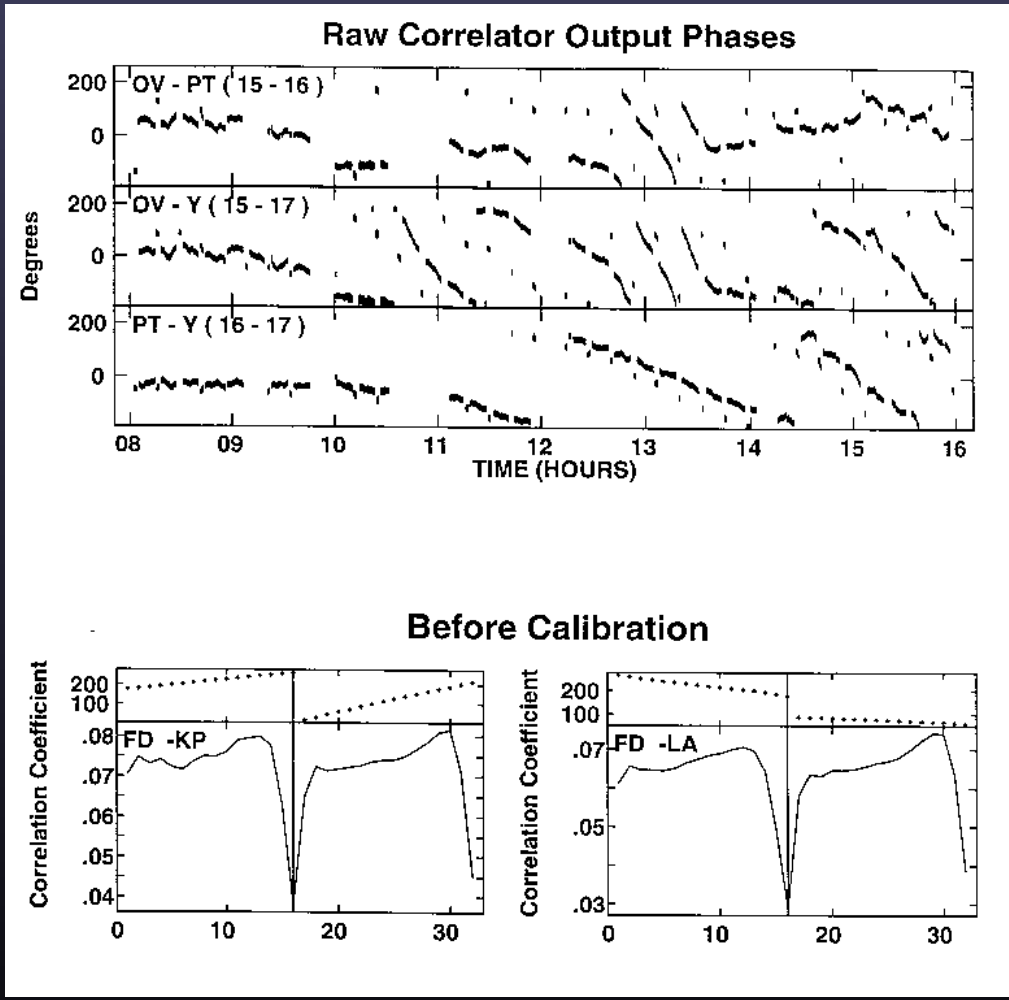

From: Ylva Pihlström, Craig Walker, Tenth Synthesis Imaging Summer School, UNM 2006.

Instrumental delays

- Caused by different signals paths through the electronics in the separate bands

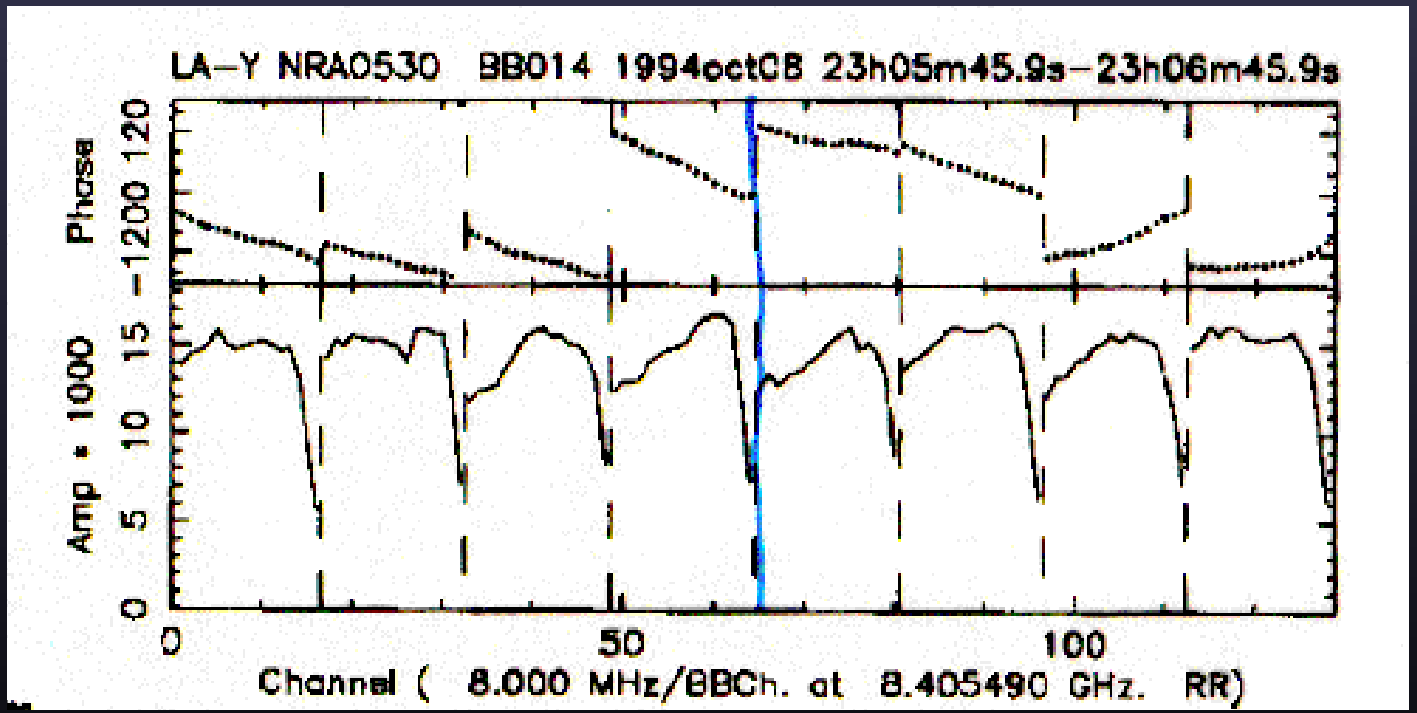

From: Ylva Pihlström, Craig Walker, Tenth Synthesis Imaging Summer School, UNM 2006.

The pulse cal

- Corrected for using the pulse cal system (continuum only)
- Tones generated by injecting a pulse every microsecond

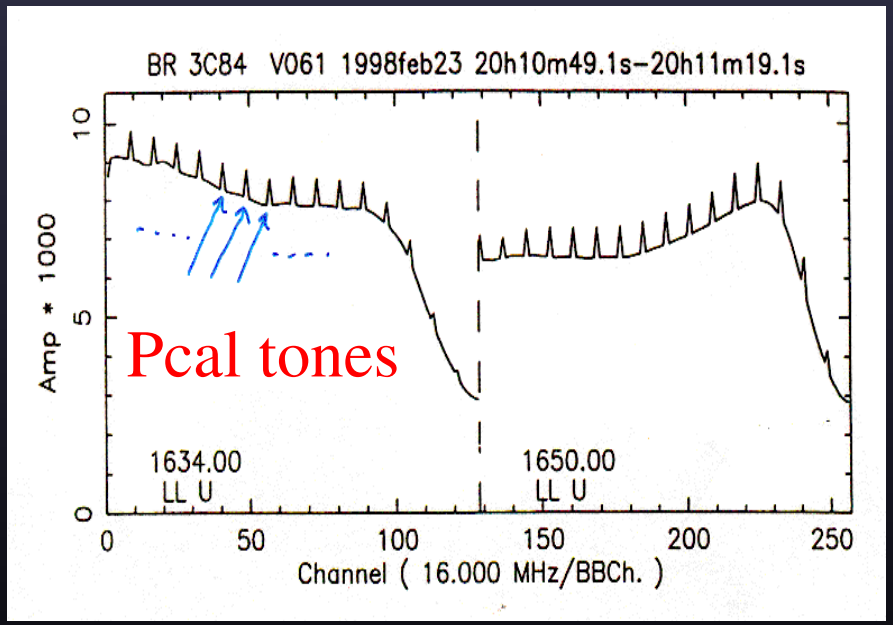

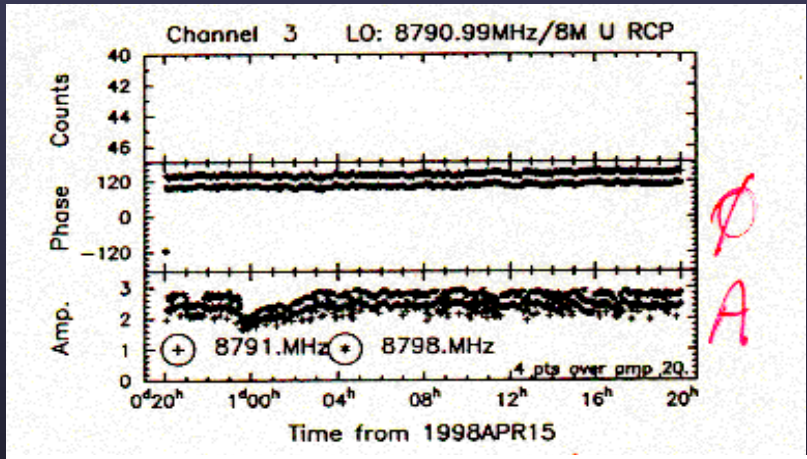

Pulse cal monitoring data

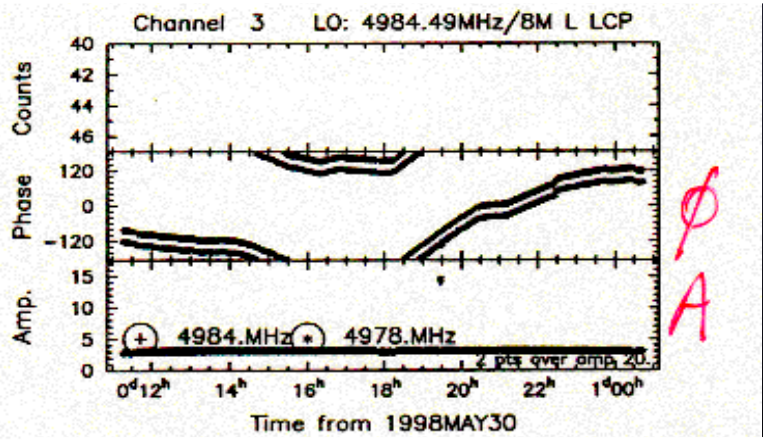

From: Ylva Pihlström, Craig Walker, Tenth Synthesis Imaging Summer School, UNM 2006.

Corrections using Pcal

- Data aligned using Pcal
- No Pcal at VLA, shows unaligned phases

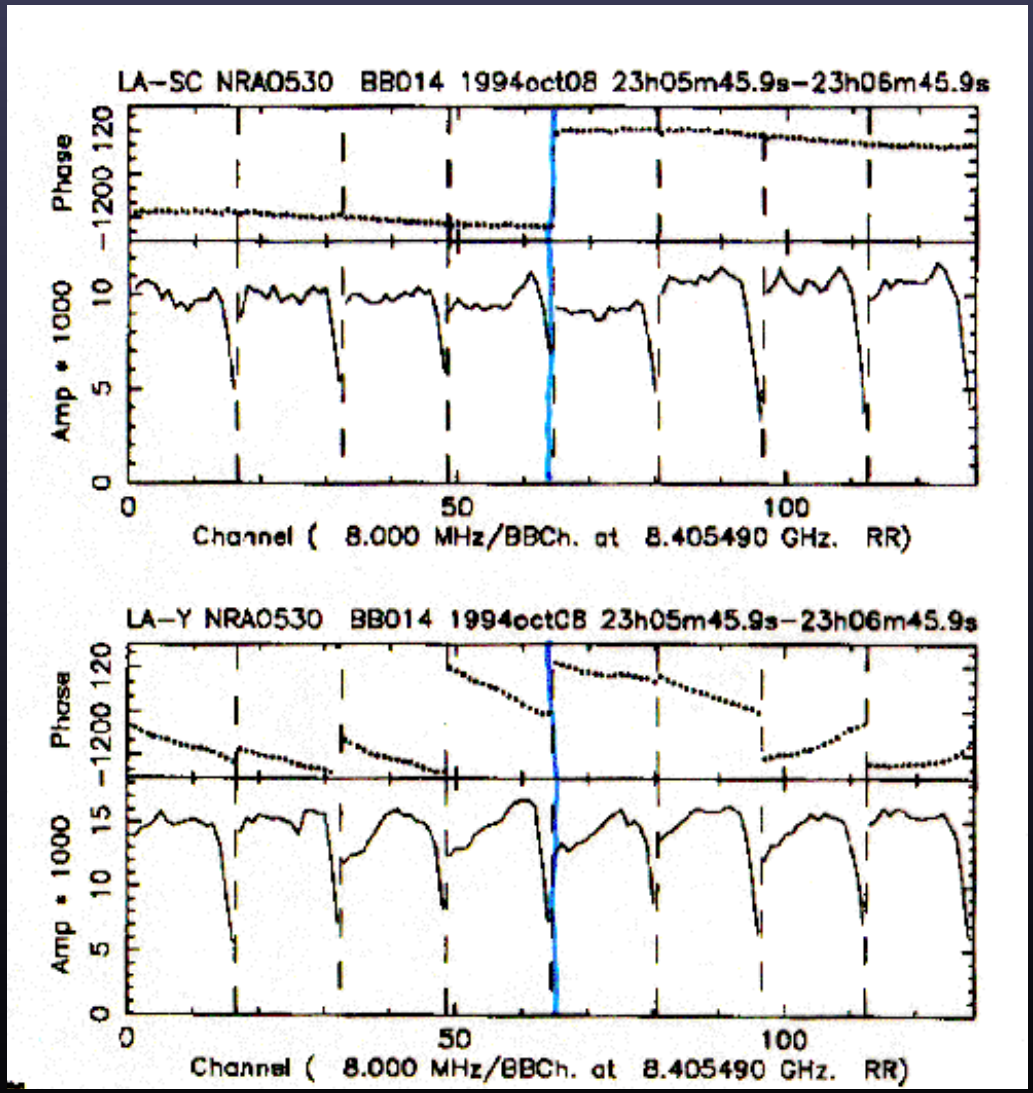

From: Ylva Pihlström, Craig Walker, Tenth Synthesis Imaging Summer School, UNM 2006.

Ionospheric delay

- Delay scales with $1/\nu^2$
- Ionosphere dominates errors at low frequencies
- Can correct with dual band observations (S/X) or GPS based models

Maximum Likely Ionospheric Contributions

Freq GHz	Day Delay ns	Night Delay ns	Day Rate mHz	Night Rate mHz
0.327	1100	110	12	1.2
0.610	320	32	6.5	0.6
1.4	60	6.0	2.8	0.3
2.3	23	2.3	1.7	0.2
5.0	5.0	0.5	0.8	0.1
8.4	1.7	0.2	0.5	0.05
15	0.5	0.05	0.3	0.03
22	0.2	0.02	0.2	0.02
43	0.1	0.01	0.1	0.01

Delays from an S/X Geodesy Observation

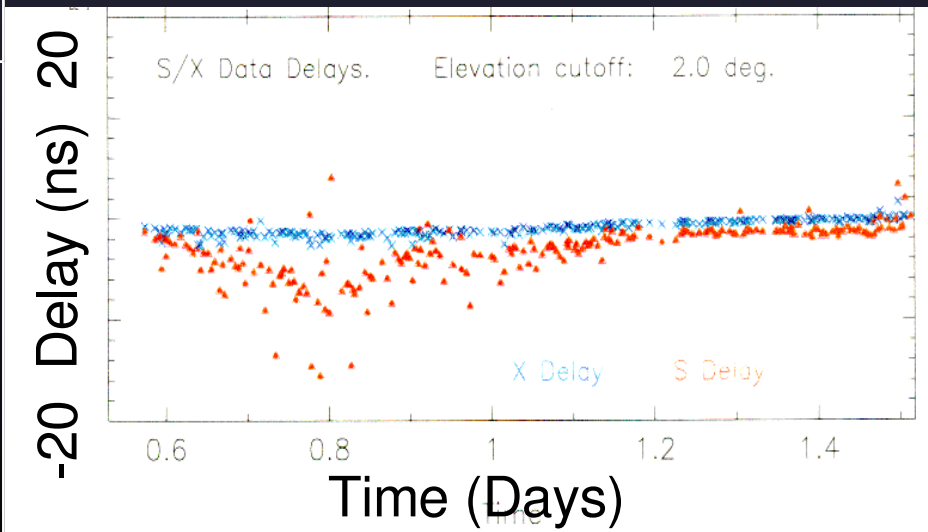

From: Ylva Pihlström, Craig Walker, Tenth Synthesis Imaging Summer School, UNM 2006.

Editing

- Flags from on-line system will remove most bad data
  - Antenna off source
  - Subreflector out of position
  - Synthesizers not locked

- Final flagging done by examining data
  - Flag by antenna (most problems are antenna based)
  - Poor weather
  - Bad playback
  - RFI (may need to flag by channel)
  - First point in scan sometimes bad

From: Ylva Pihlström, Craig Walker, Tenth Synthesis Imaging Summer School, UNM 2006.

Editing example

Raw Data - No Edits

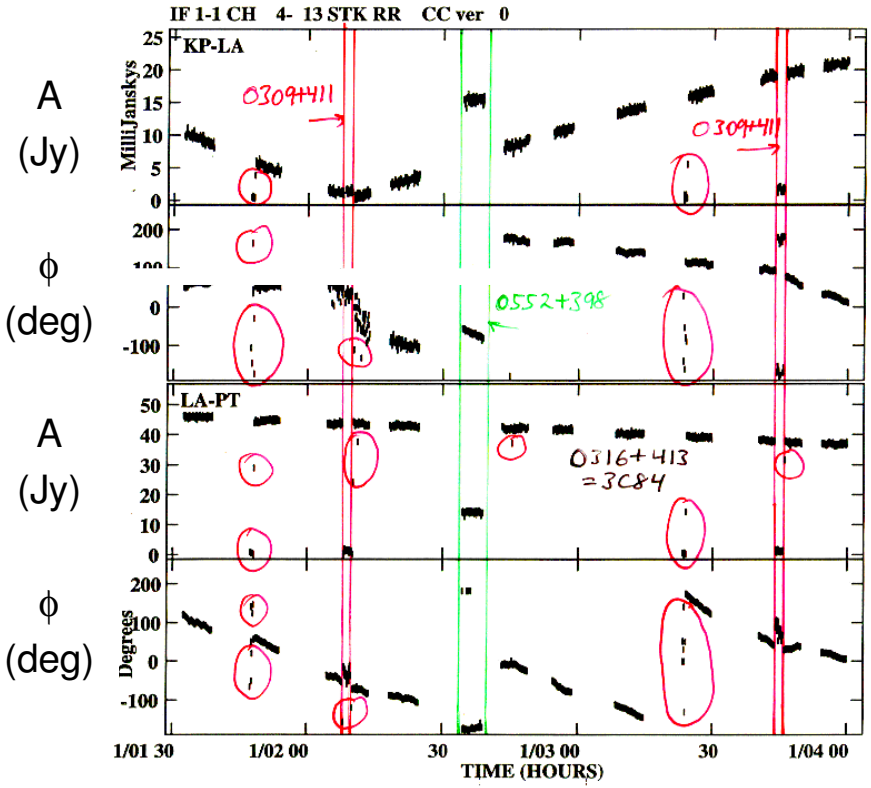

Raw Data - Edited

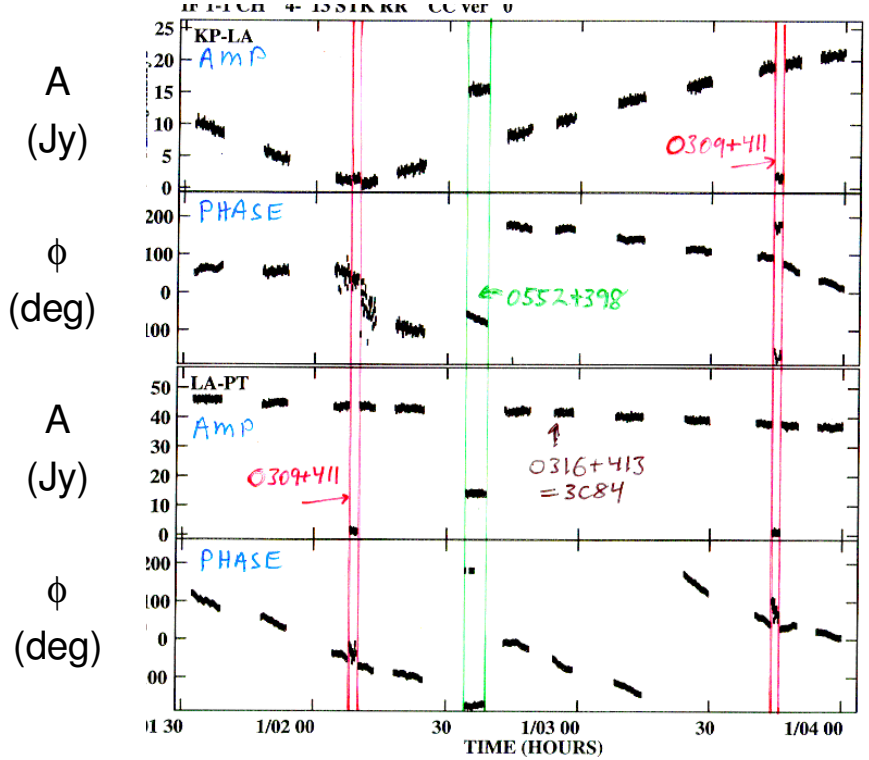

From: Ylva Pihlström, Craig Walker, Tenth Synthesis Imaging Summer School, UNM 2006.

Phase errors

- Raw correlator output has phase slopes in time and frequency
- Caused by imperfect delay model
- Need to find delay and delay-rate errors

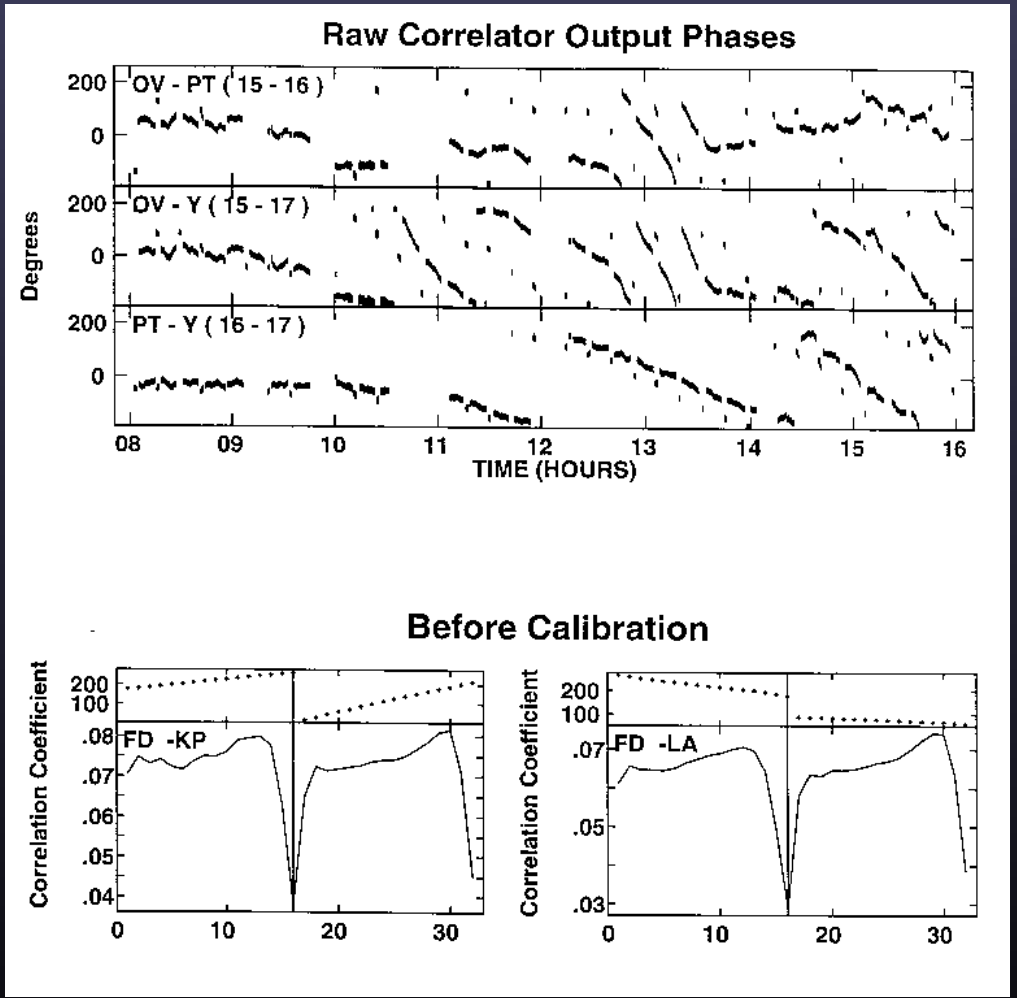

From: Ylva Pihlström, Craig Walker, Tenth Synthesis Imaging Summer School, UNM 2006.

Fringe fitting

- For astronomy:
  - Remove clock offsets and align baseband channels (“manual pcal”)
  - Fit calibrator to track most variations
  - Fit target source if strong
  - Used to allow averaging in frequency and time
    - Allows higher SNR self calibration (longer solution, more bandwidth)

- For geodesy:
  - Fitted delays are the primary “observable”
  - Correlator model is added to get “total delay”, independent of models

From: Ylva Pihlström, Craig Walker, Tenth Synthesis Imaging Summer School, UNM 2006.

Delay and rate

Phase due delay and rate:

$$\Delta\phi_{t,\nu} = \phi_0 + \left(\frac{\partial\phi}{\partial\nu}\Delta\nu + \frac{\partial\phi}{\partial t}\Delta t\right) \tag{9}$$

Delay and rate

Phase due delay and rate:

$$\Delta\phi_{t,\nu} = \phi_0 + \left(\frac{\partial\phi}{\partial\nu}\Delta\nu + \frac{\partial\phi}{\partial t}\Delta t\right) \tag{9}$$

Baseline phase errors due to delay and rate:

$$\Delta\phi_{ij} = \phi_{i0} - \phi_{j0} + \left(\left[\frac{\partial\phi_i}{\partial\nu} - \frac{\partial\phi_j}{\partial\nu}\right]\Delta\nu + \left[\frac{\partial\phi_i}{\partial t} - \frac{\partial\phi_j}{\partial t}\right]\Delta t\right) \tag{10}$$

Fringe fitting and self calibration

Delays, rates, and phases are usually solved for antennas not for baselines, this is called *global fringe fitting* and gives better sensitivity (all data for a given antenna is used). In some special cases *baseline based* fringe fitting is used.

In both methods, the source is assumed to be point-like (constant phases and amplitudes), if not, a model for the source can be used.

Self calibration is solving the *antenna phases* and sometimes amplitudes (not visibility phases!!) based on a source model.

Self calibration imaging sequence

- Iterative procedure to solve for both image and gains:
  - Use best available image to solve for gains (start with point)
  - Use gains to derive improved image
  - Should converge quickly for simple sources
- Does not preserve absolute position or flux density scale

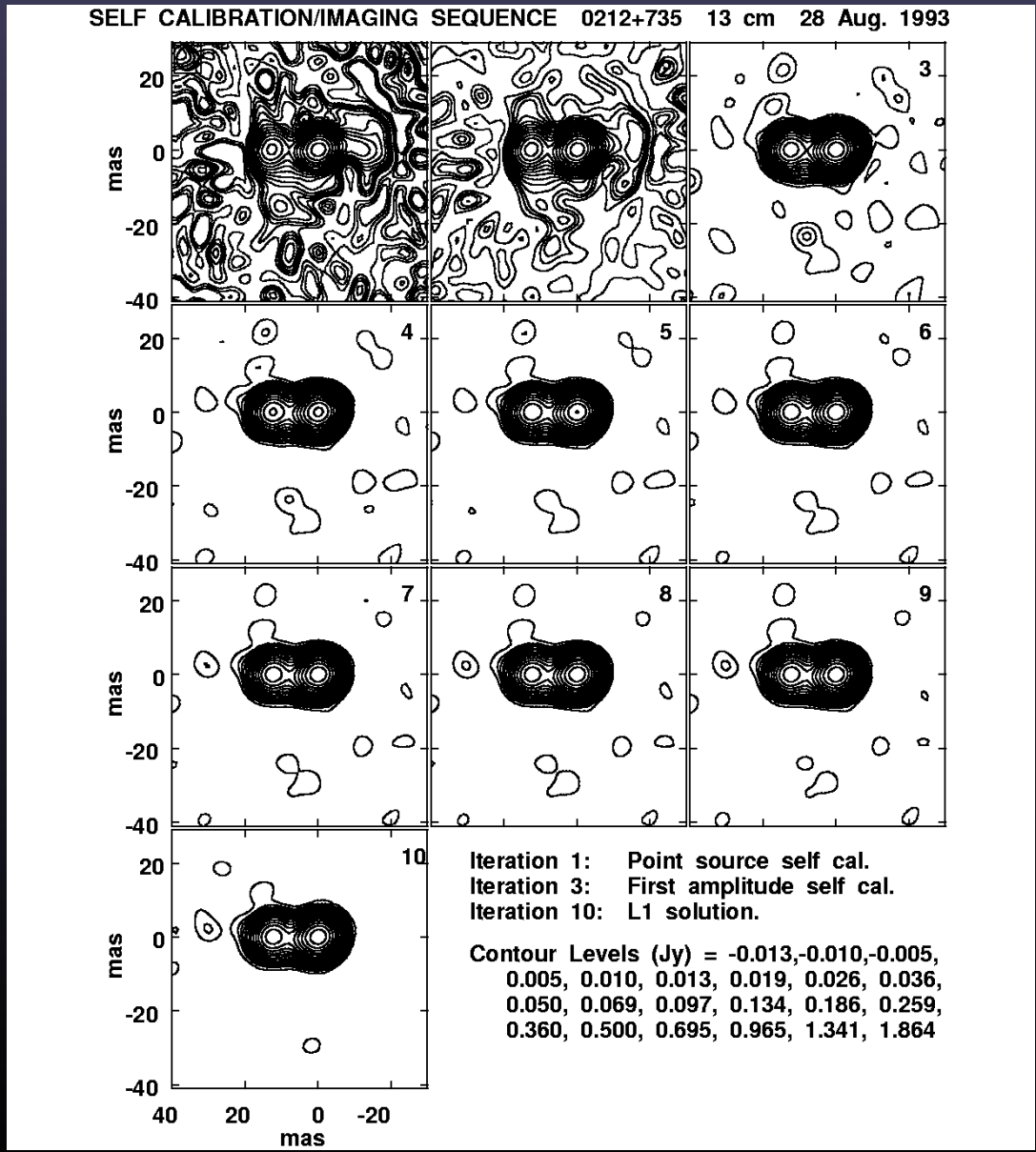

From: Ylva Pihlström, Craig Walker, Tenth Synthesis Imaging Summer School, UNM 2006.

Closure phases I

The phase of a baseline consists of three components:

$$\phi_{ij} = \phi_{ij}^{\text{true}} + \phi_i^{\text{err}} - \phi_j^{\text{err}}, \tag{11}$$

i.e true phase due to the source structure and phase errors of individual antennas.

Closure phases I

The phase of a baseline consists of three components:

$$\phi_{ij} = \phi_{ij}^{\text{true}} + \phi_i^{\text{err}} - \phi_j^{\text{err}}, \tag{11}$$

i.e true phase due to the source structure and phase errors of individual antennas.

If we take a sum of phases of three antennas, or a baseline triangle, we get the closure phase:

$$\begin{aligned}\Psi_{ijk} &= \phi_{ij} + \phi_{jk} + \phi_{ki} \\ &= (\phi_{ij}^{\text{true}} + \phi_i^{\text{err}} - \phi_j^{\text{err}}) \\ &+ (\phi_{jk}^{\text{true}} + \phi_j^{\text{err}} - \phi_k^{\text{err}}) \\ &+ (\phi_{ki}^{\text{true}} + \phi_k^{\text{err}} - \phi_i^{\text{err}})\end{aligned}$$

Closure phases II

The phase-error of the second antenna is negative because visibilities are Hermitian i.e. when you swap antennas, the visibility is a complex conjugate of the original.

Closure phases II

The phase-error of the second antenna is negative because visibilities are Hermitian i.e. when you swap antennas, the visibility is a complex conjugate of the original.
Rearranging:

$$\begin{aligned}\Psi_{ijk} = \phi_{ij}^{\text{true}} + \phi_{jk}^{\text{true}} + \phi_{ki}^{\text{true}} \\ + \phi_{i}^{\text{err}} - \phi_{i}^{\text{err}} \\ + \phi_{j}^{\text{err}} - \phi_{j}^{\text{err}} \\ + \phi_{k}^{\text{err}} - \phi_{k}^{\text{err}}.\end{aligned}$$

Closure phases II

The phase-error of the second antenna is negative because visibilities are Hermitian i.e. when you swap antennas, the visibility is a complex conjugate of the original.
Rearranging:

$$\begin{aligned}\Psi_{ijk} = \phi_{ij}^{\text{true}} + \phi_{jk}^{\text{true}} + \phi_{ki}^{\text{true}} \\ + \phi_{i}^{\text{err}} - \phi_{i}^{\text{err}} \\ + \phi_{j}^{\text{err}} - \phi_{j}^{\text{err}} \\ + \phi_{k}^{\text{err}} - \phi_{k}^{\text{err}}.\end{aligned}$$

$$\Psi_{ijk} = \phi_{ij}^{\text{true}} + \phi_{jk}^{\text{true}} + \phi_{ki}^{\text{true}} \tag{12}$$

I.e. all **antenna based** errors are cancelled. Closure phase is actually a complex quantity called the *triple product* or *bispectrum*.

SMA closure phase measurements at 682GHz

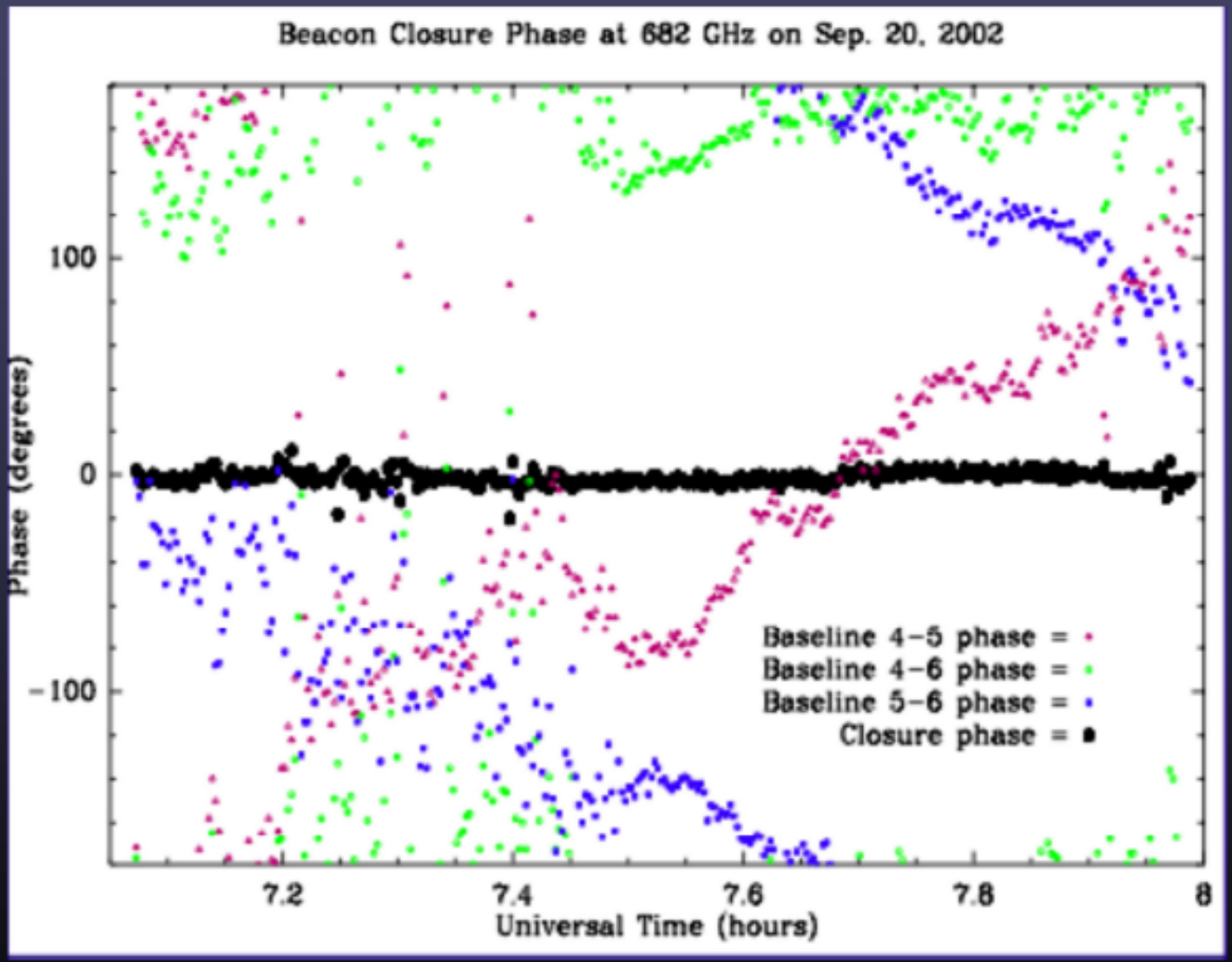

From: Rupen, Tenth Summer Synthesis Imaging Workshop, University of New Mexico, Jun 13-20, 2006

Imaging

There are three basic methods to produce images from interferometry data:

- Fitting a source model to the visibilities.
  - Possible to get images even from a noisy and sparse dataset.
  - Accurate source parameters: emission component sizes, shapes, and locations.
- Inverse transform of the visibilities and deconvolution.
  - No a-priori control of source shape $\Rightarrow$ somewhat more objective approach.
  - Clean (many variants), maximum entropy method (MEM) most important deconvolution methods.
- Direct inversion using **Compressed Sensing** algorithms (in development)

Inspecting visibility data

Before imaging it is very useful to make plots of visibility phase and amplitude:

- vs. uv-radius
- vs. time
- vs. uv-projection (slice across the uv-plane)

UV-coverage (sampling) map tells the general quality that is to be expected (sidelobe/artifact level).

These plots give first ideas what to expect from the source structure.

Sampling of the (u,v) plane

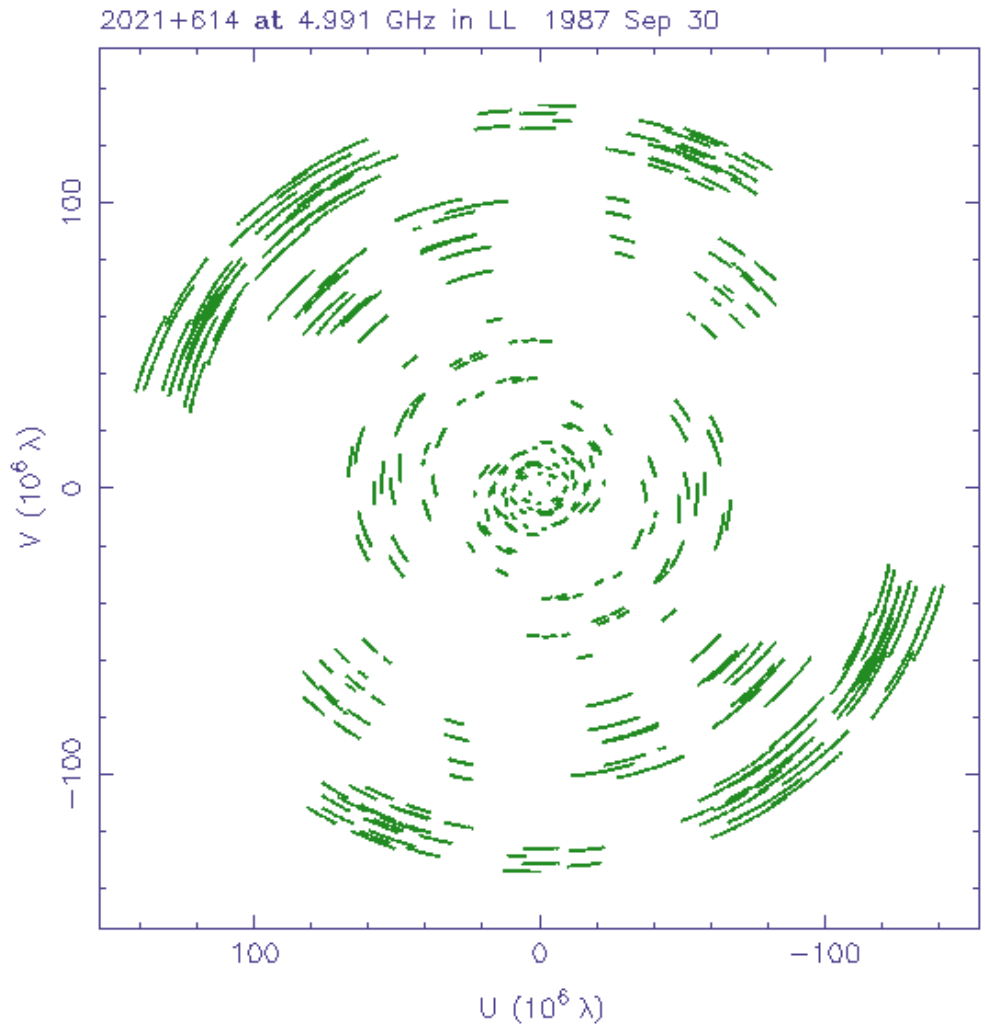

Visibility versus (u,v) radius

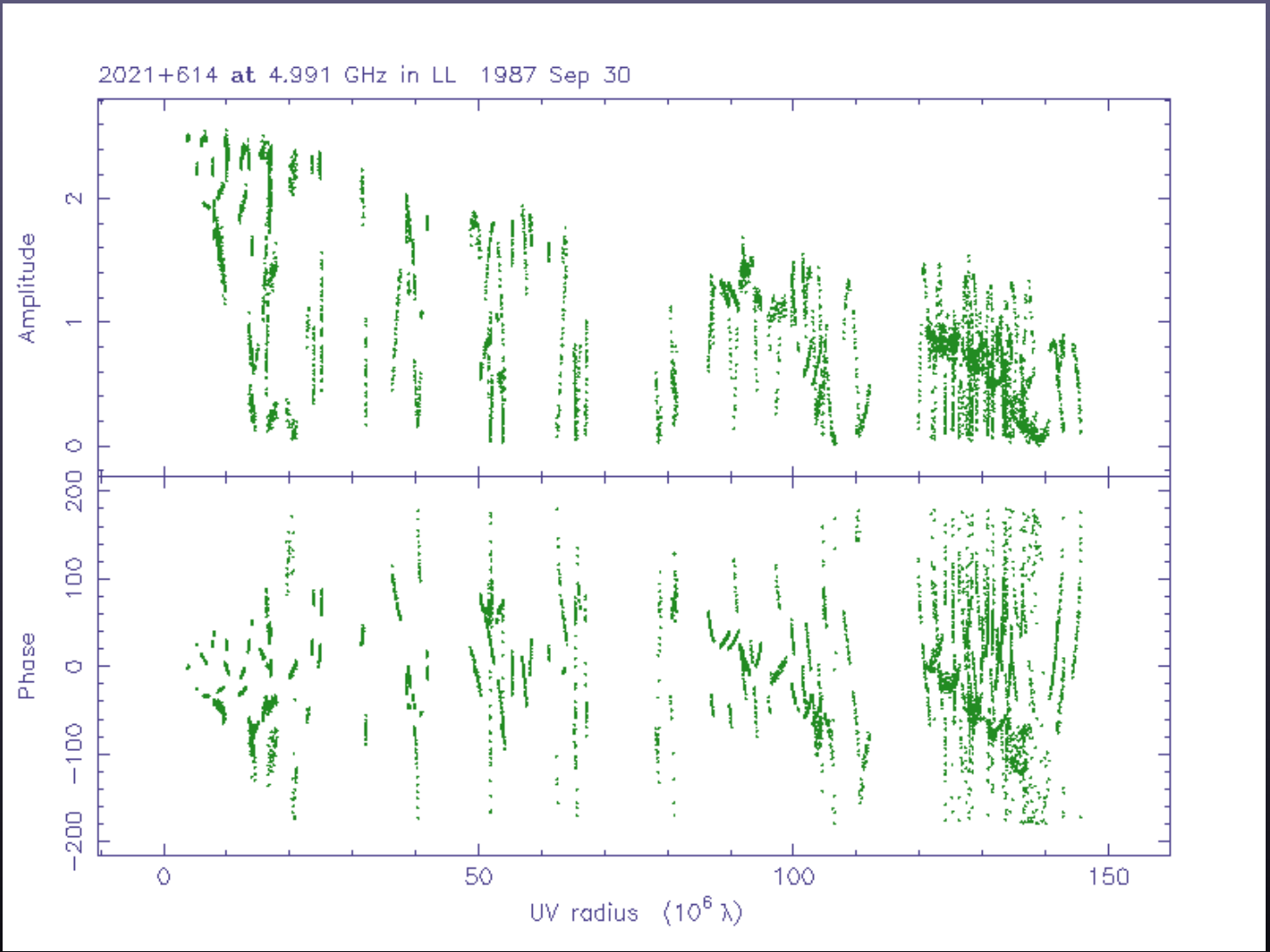

Visibility versus time

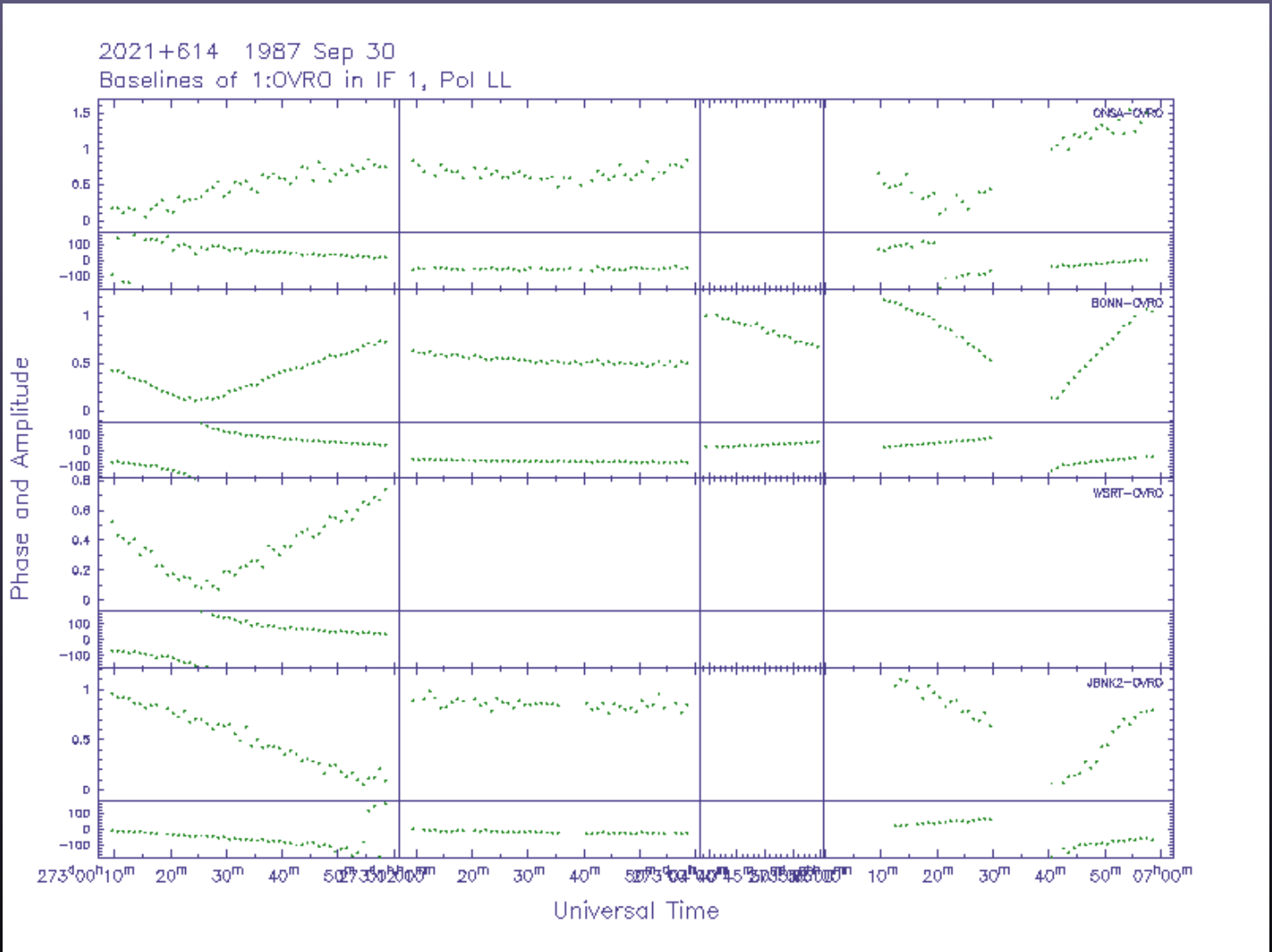

Amplitude across the (u,v) plane

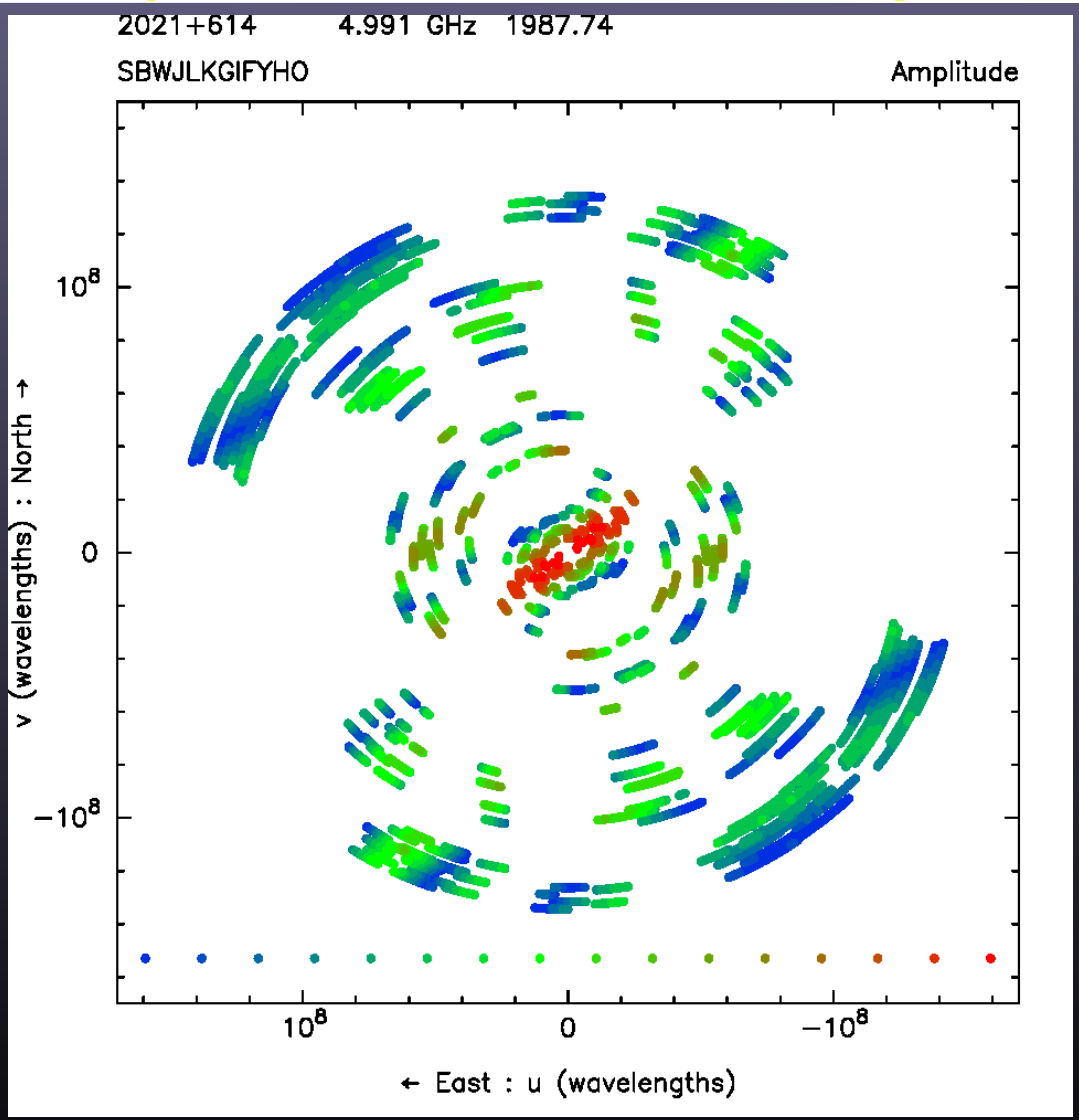

Projection in the (u,v) plane

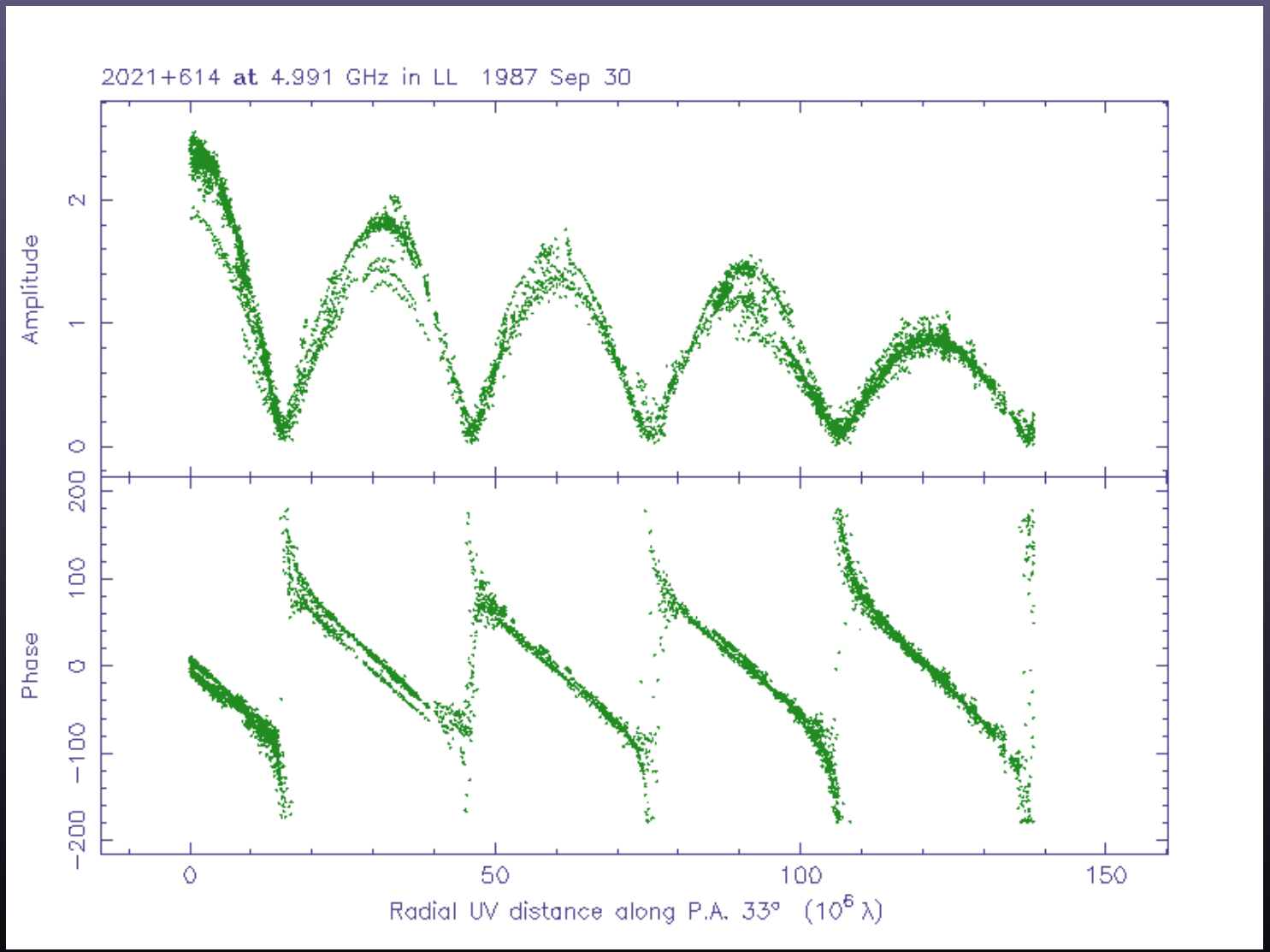

Fourier transform properties

$$F(u,v) = \mathrm{FT}\{f(x,y)\}$$

i.e.,

$$F(u,v) = \int_{-\infty}^{\infty}\int_{-\infty}^{\infty} f(x,y)\exp[2\pi i(ux+vy)]\,dx\,dy$$

Linearity

$$\mathrm{FT}\{f(x,y)+g(x,y)\} = F(u,v)+G(u,v)$$

Convolution

$$\mathrm{FT}\{f(x,y)\star g(x,y)\} = F(u,v)\cdot G(u,v)$$

Shift

$$\mathrm{FT}\{f(x-x_i,y-y_i)\} = F(u,v)\ \exp[2\pi i(ux_i+vy_i)]$$

Similarity

$$\mathrm{FT}\{f(ax,by)\} = \frac{1}{|ab|}F\left(\frac{u}{a},\frac{v}{b}\right)$$

Simple source structures

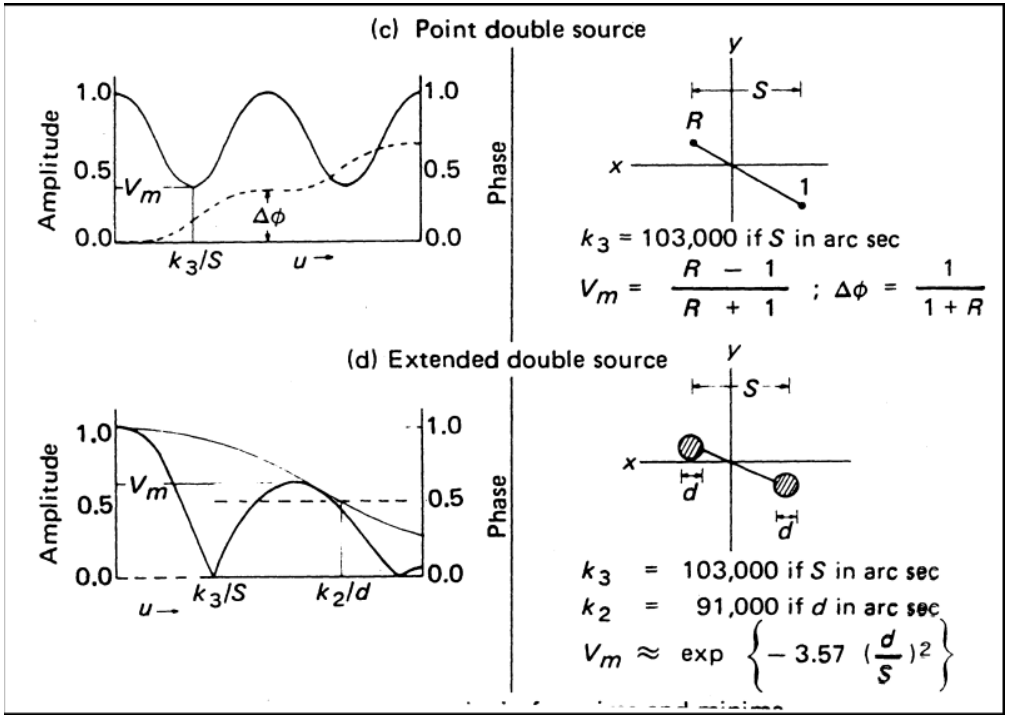

Component separation from the uv-radius (in wavelengths) of the first valley (k3/S), size of individual emission region (d [arcsec]) from the uv-radius of the half-value point of the envelope (k2/d). Amplitude is normalized.

Simple source structures, example

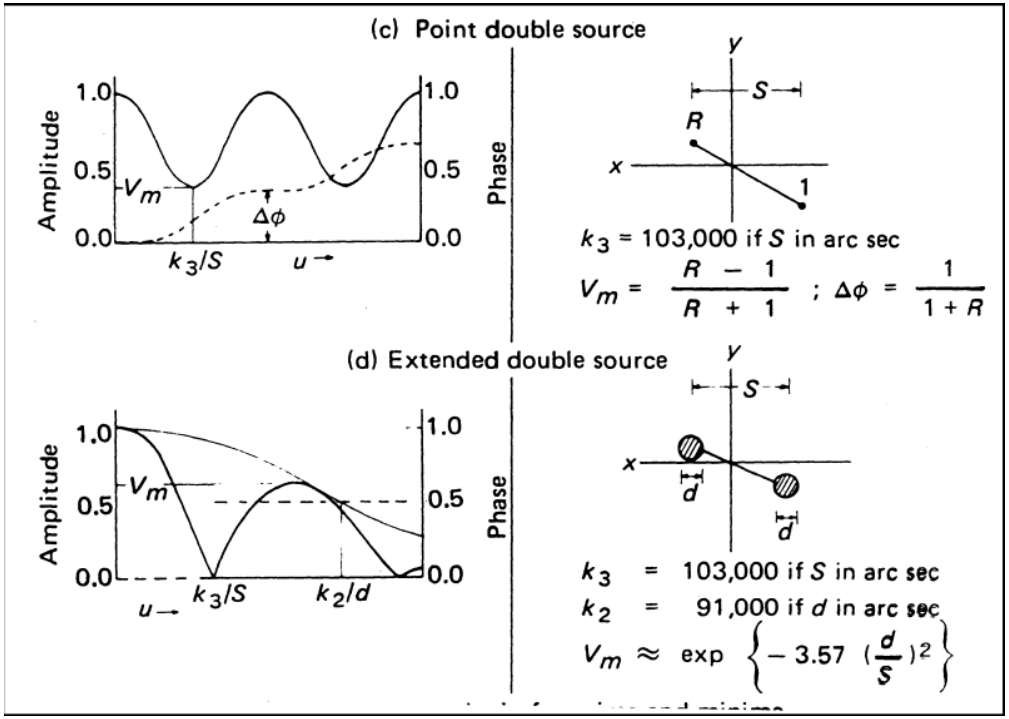

First valley at 100 M$\lambda = k_3/S$, envelope half-value point 300 M$\lambda = k_2/d$.

Double source, component separation

$S = k3/100\mathrm{M}\lambda = 103000/100e6 = 0.001\,\mathrm{arcsec} = 1\,\mathrm{marcsec}.$

Component size

$d = k2/300\mathrm{M}\lambda = 91000/300e6 = 0.0003\,\mathrm{arcsec} = 300\,\mu\mathrm{arcsec}$

Simple source structures in 2D

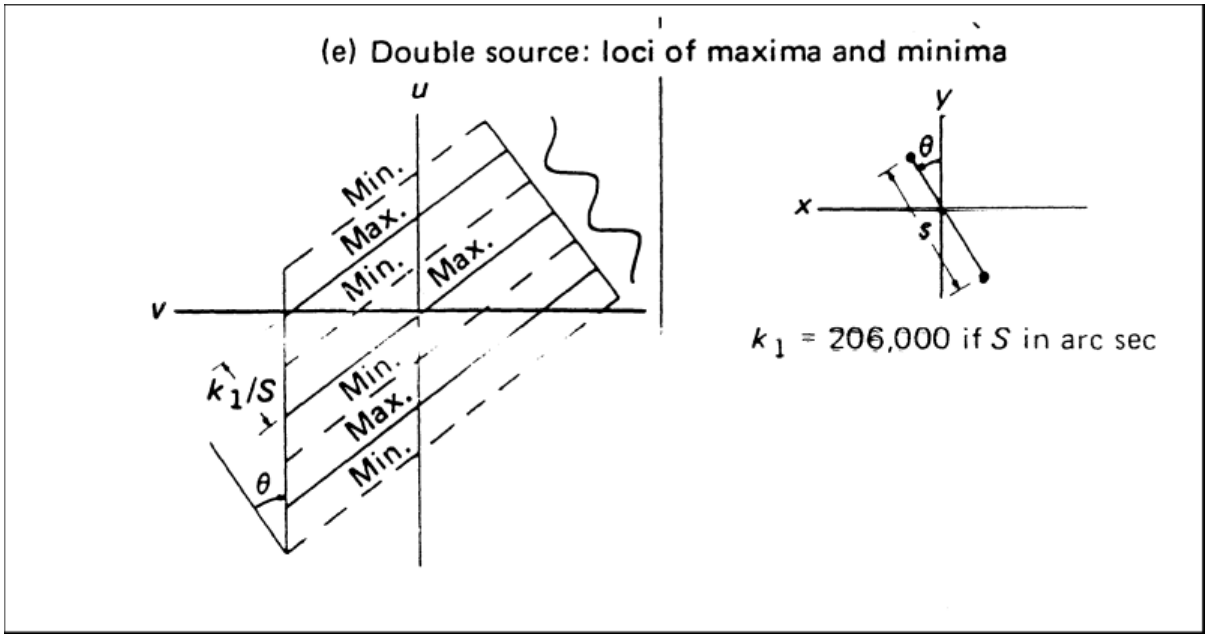

Component separation from the valley-to-valley distance (k1/S).

Source shift

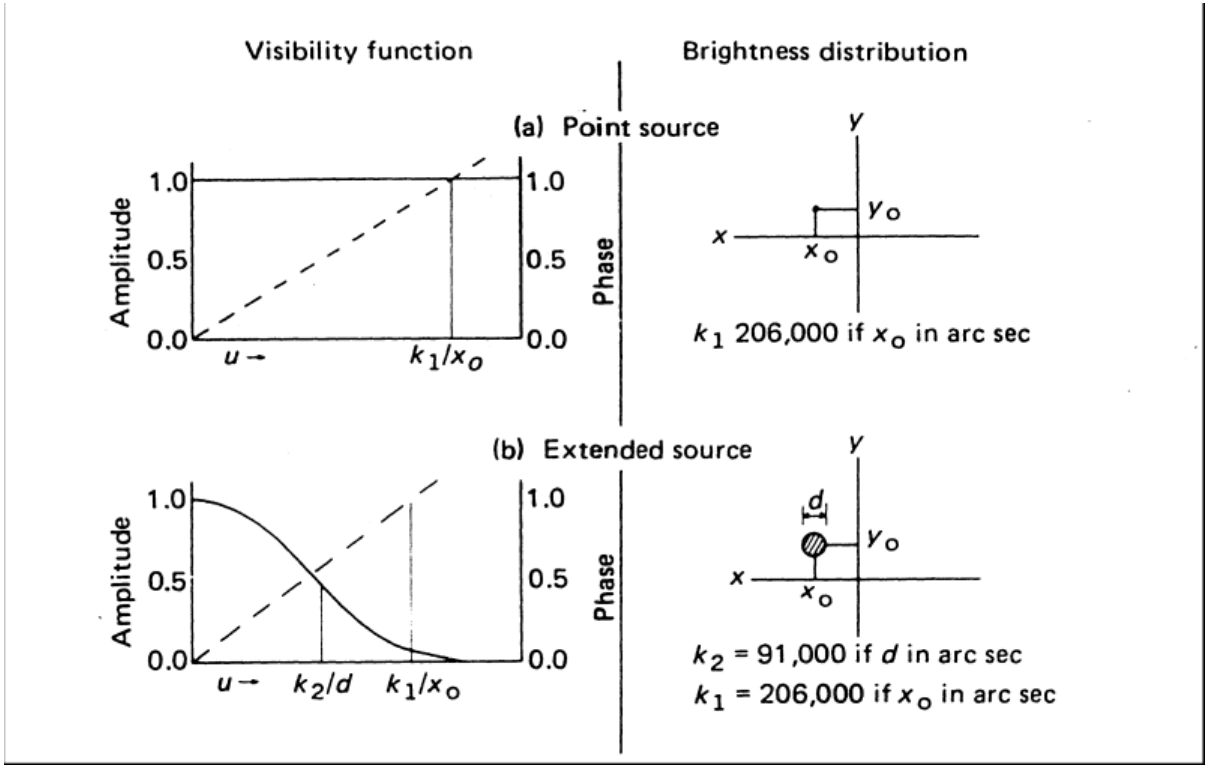

Component profiles

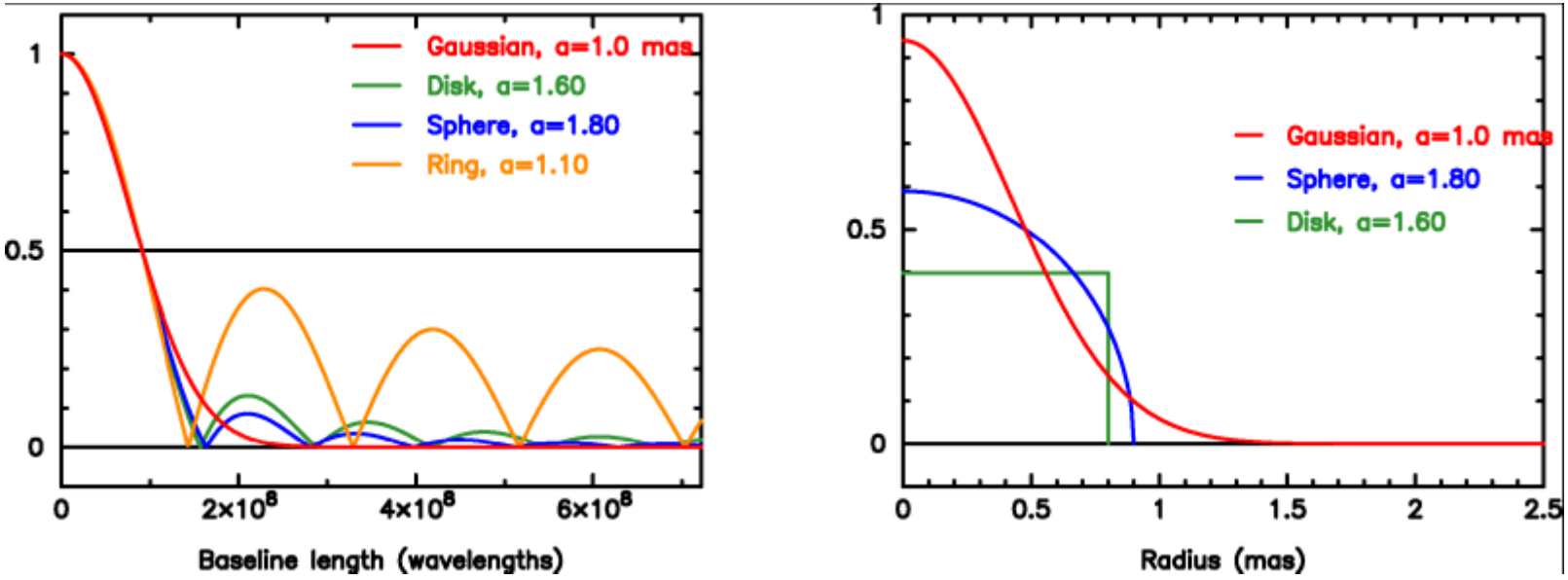

There is very little difference in the uv-plane between different source profiles down to the relative half flux level.

Trial model

- By inspection, we can derive a simple model:
- Two equal components, each 1.25 Jy, separated by about 6.8 milliarcsec in p.a. 33º, each about 0.8 milliarcsec in diameter (Gaussian FWHM)
- *To be refined later.*

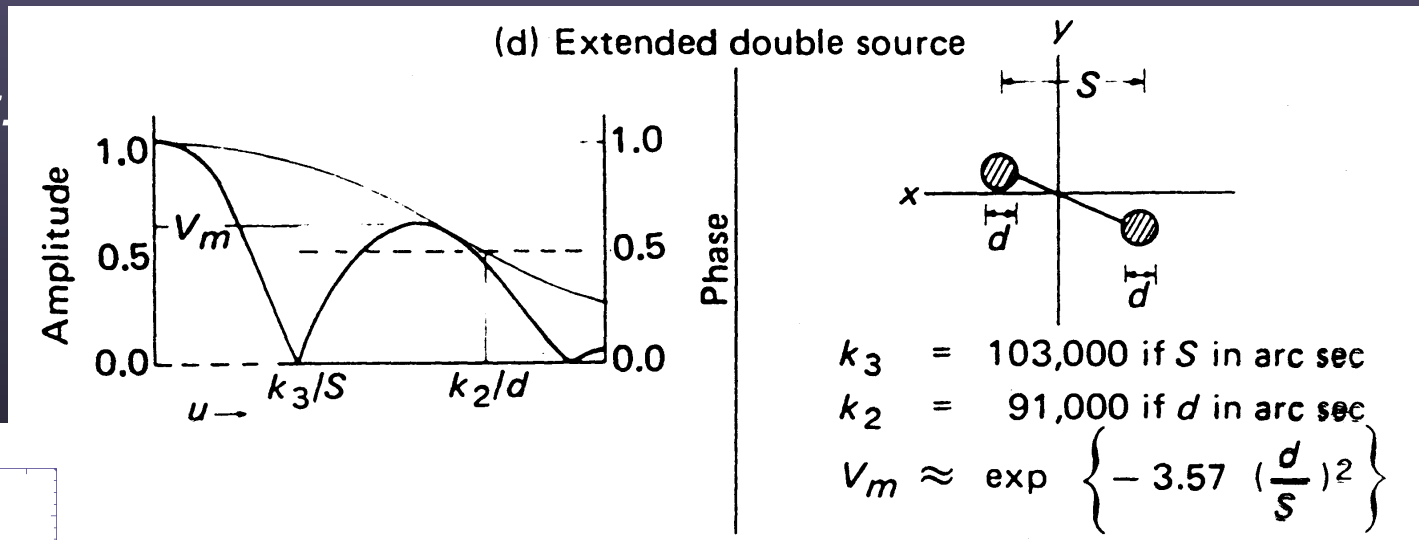

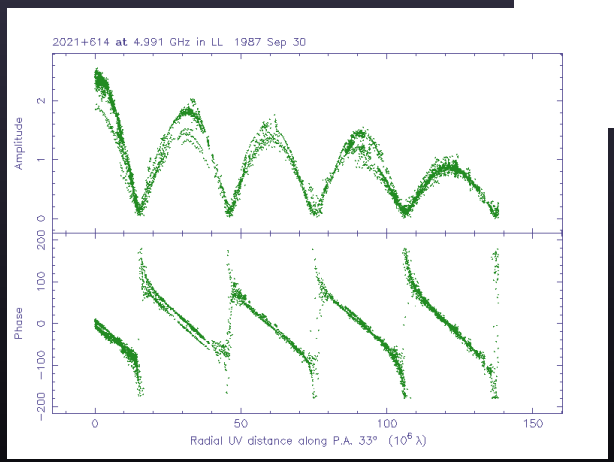

Projection in the (u,v) plane

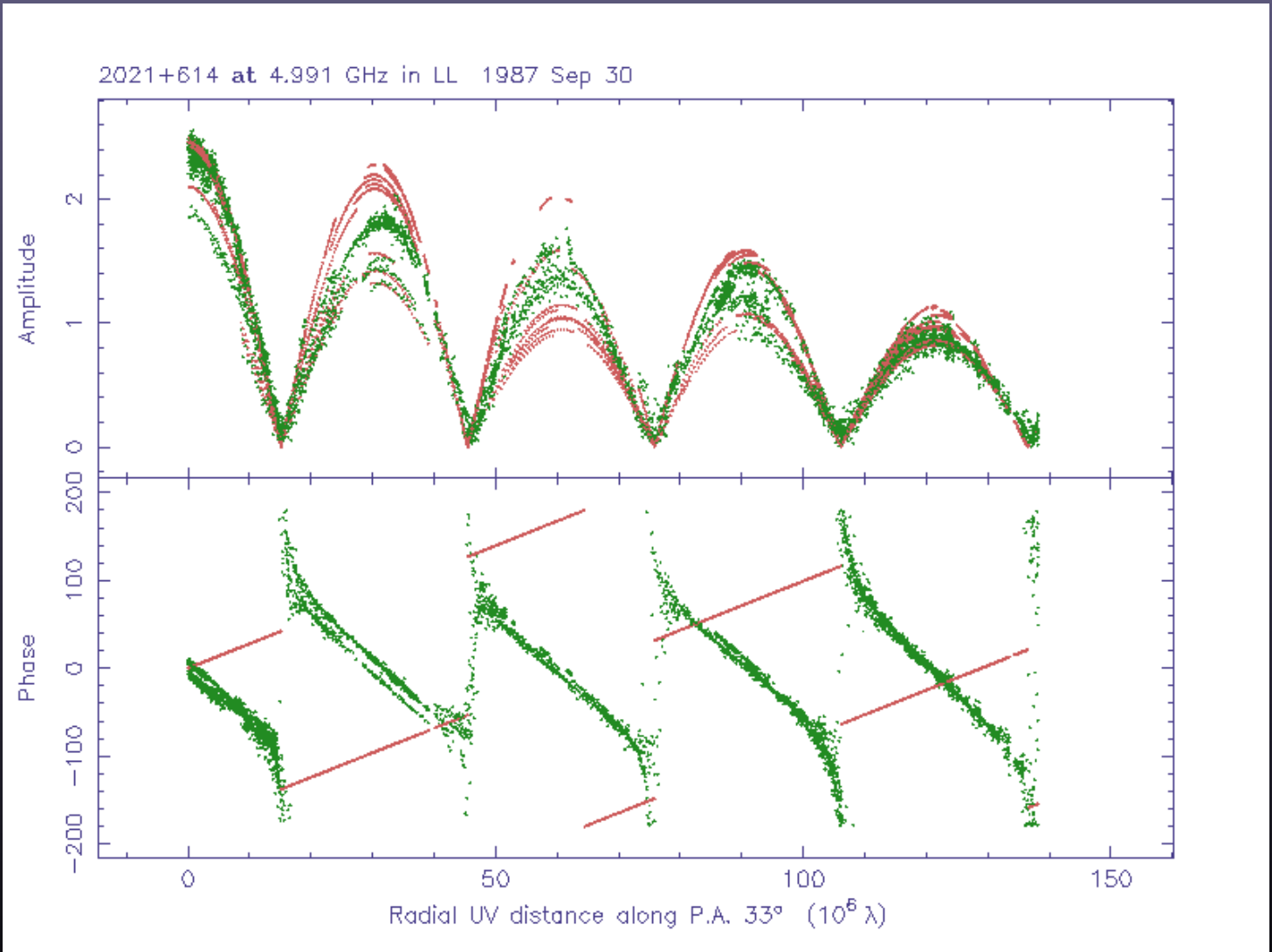

Parameters

- Example
  - Component position: (*x,y*) or polar coordinates
  - Flux density
  - Angular size (e.g., FWHM)
  - Axial ratio and orientation (position angle)
    - For a non-circular component
  - 6 parameters per component, plus a “shape”

  - This is a conventional choice: other choices of parameters may be better!
  - (Wavelets; shapelets* [Hermite functions])
    - * Chang & Refregier 2002, ApJ, 570, 447

Practical model fitting: 2021

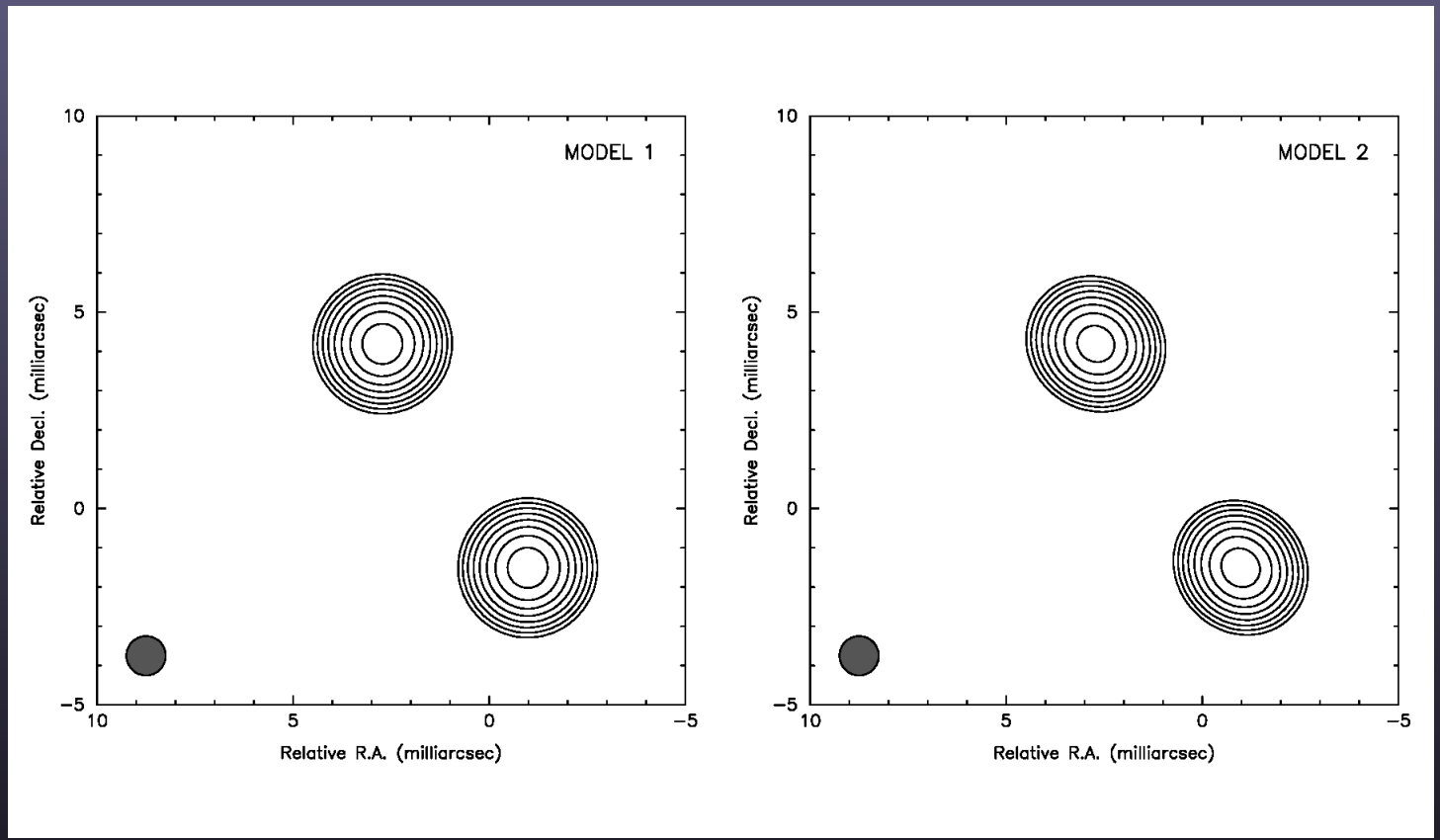

- ! Flux (Jy) Radius (mas) Theta (deg) Major (mas) Axial ratio Phi (deg) T
- 1.15566 4.99484 32.9118 0.867594 0.803463 54.4823 1
- 1.16520 1.79539 -147.037 0.825078 0.742822 45.2283 1

2021: model 2

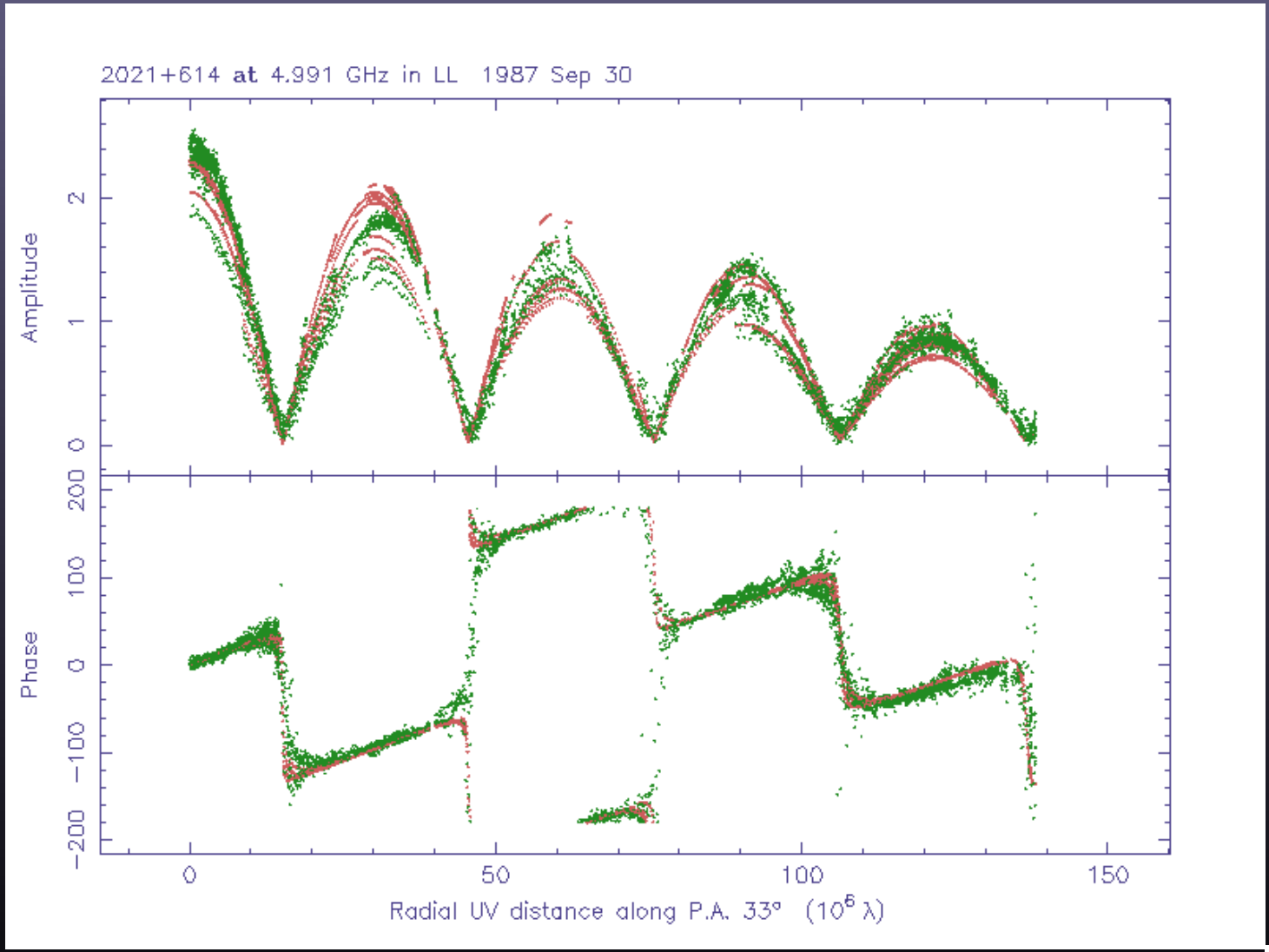
2021+614 at 4.991 GHz in LL 1987 Sep 30
Amplitude
0
1
2
Phase
200
100
0
−100
−200
0
50
100
150
Radial UV distance along P.A. 33° (10^6 λ)

Model fitting 2021

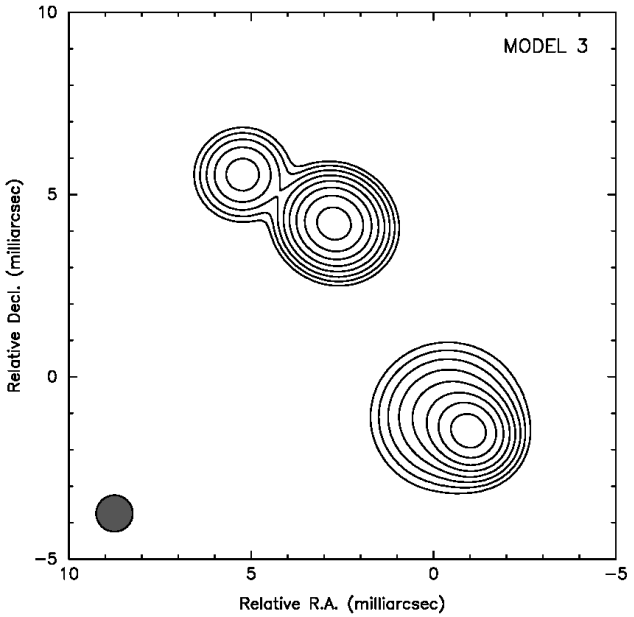

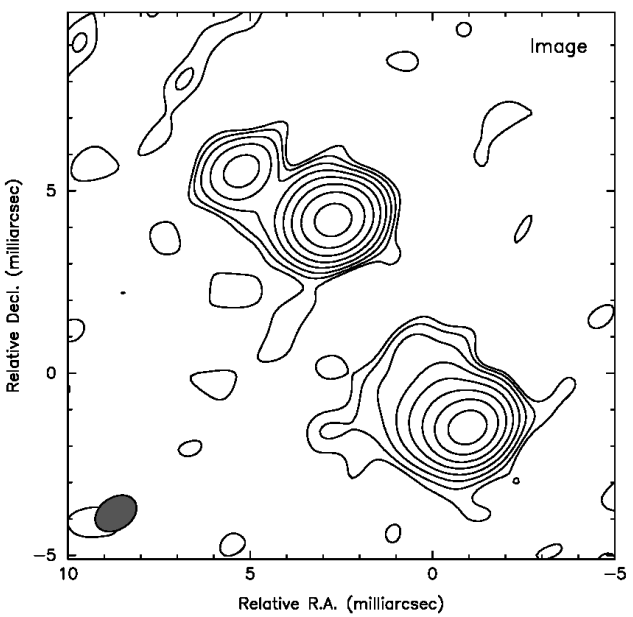

! Flux (Jy)	Radius (mas)	Theta (deg)	Major (mas)	Axial ratio	Phi (deg)	T
1.10808	5.01177	32.9772	0.871643	0.790796	60.4327	1
0.823118	1.80865	−146.615	0.589278	0.585766	53.1916	1
0.131209	7.62679	43.3576	0.741253	0.933106	−82.4635	1
0.419373	1.18399	−160.136	1.62101	0.951732	84.9951	1

2021: model 3

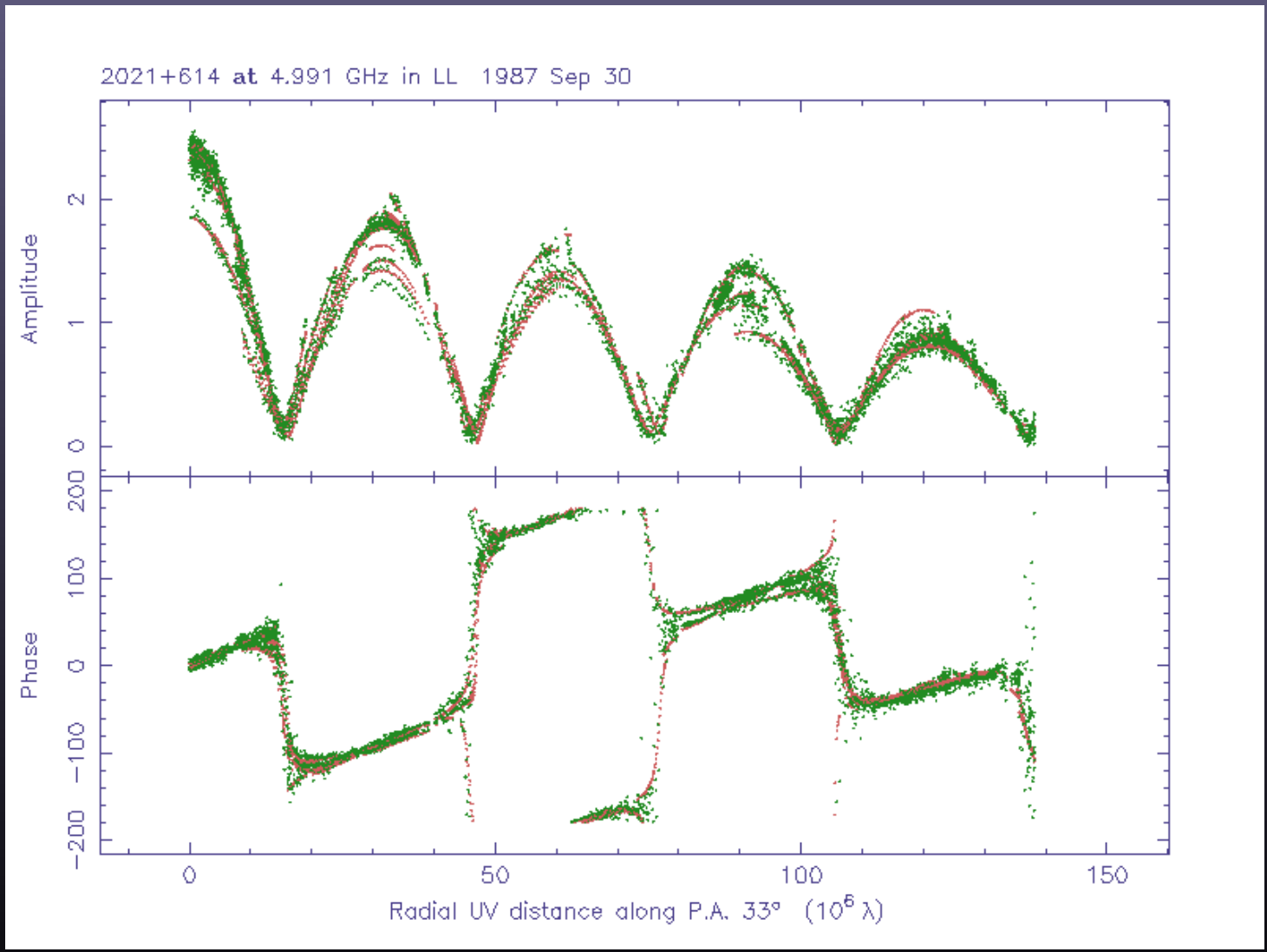
2021+614 at 4.991 GHz in LL 1987 Sep 30
Amplitude
2
1
0
Phase
200
100
0
−100
−200
0
50
100
150
Radial UV distance along P.A. 33° (10^6 λ)

Applications: A Binary Star

- Binary Stars
  - Many stars are in binary systems
  - Orbital parameters can be used to measure stellar masses
  - Astrometry can provide direct distances via parallax and proper motions.
- Application of model fitting
  - Optical interferometry provides sparse visibility coverage
  - Small number of components
  - Need error estimates.
- Example: NPOI observations of Phi Herculis (Zavala et al. 2006)
  - Multiple observations map out the orbit

NPOI = Navy Precision Optical Interferometer, three arm 'Y', 250 m each.

NPOI Observations of Phi Her

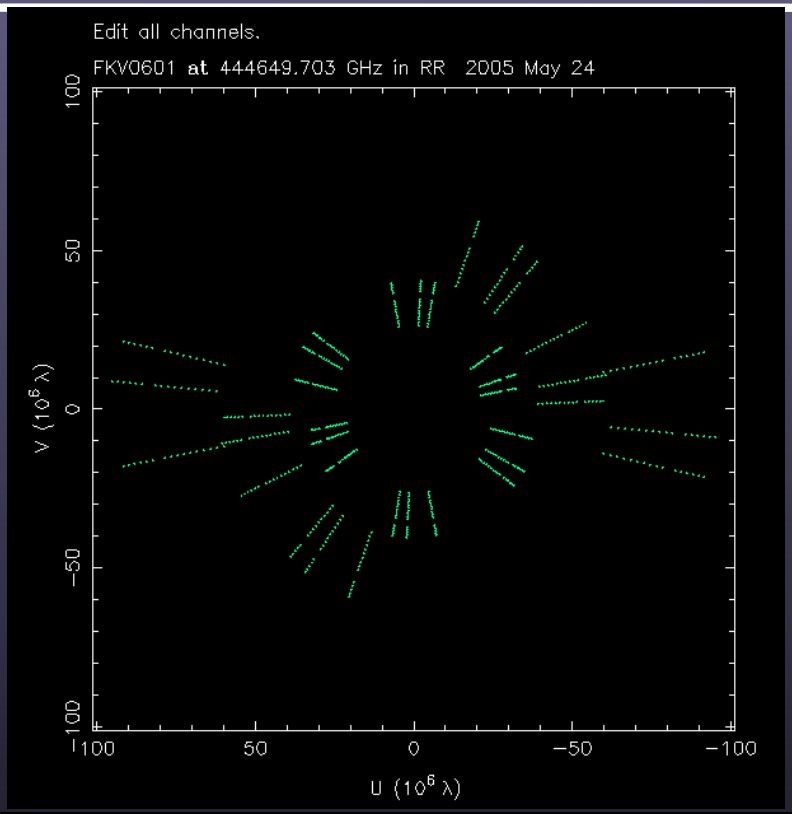

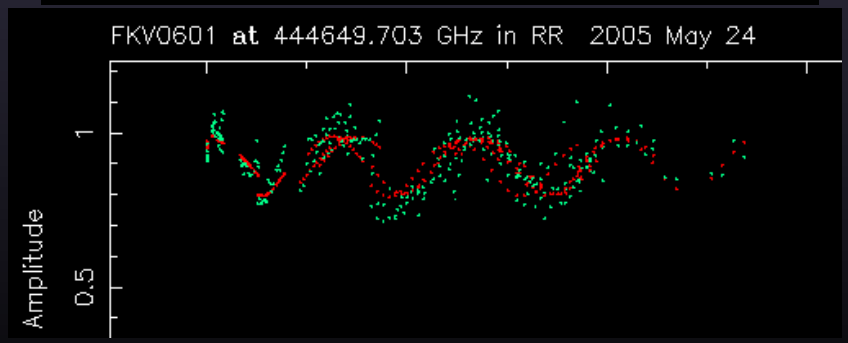

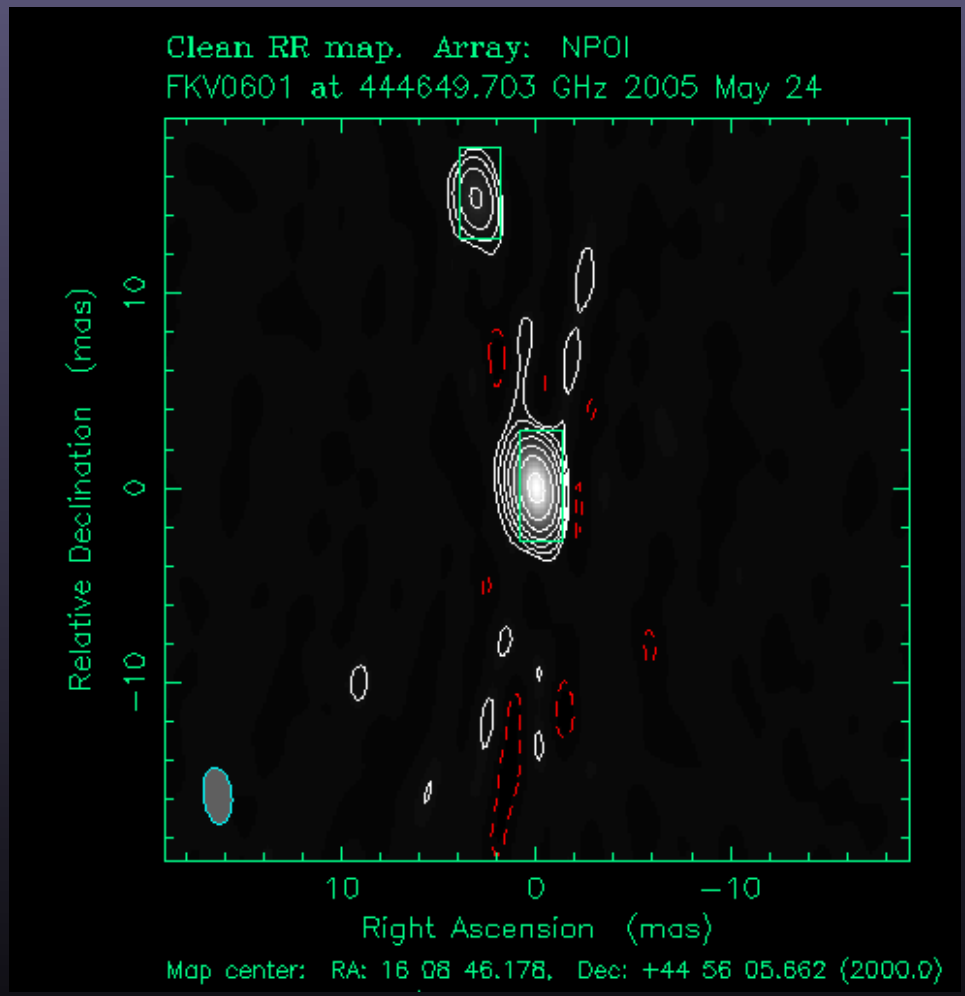

Deconvolution

- If the whole uv-plane would be sampled, a simple Fourier inverse transform would be enough to make images.
- Dirty image is a convolution between ideal image and the PSF (dirty beam).
- The missing information must be interpolated (and sometimes extrapolated) to avoid sidelobes/artefacts.
- Especially the 'central hole' of the uv-plan can be filled using single-dish low-resolution maps.
- Fortunately external 'known' information can be used to fill the voids:
  - Flux is positive.
  - Sky is smooth in general.
  - Sky is a collection of rather compact emission regions.

Weighting methods

Uv-data is normally weighted before inversion and deconvolution:

- Uniform weighting: $W_k = 1/\rho(u_k, v_k)$, where $\rho(u_k, v_k)$ is the density of points in the k^{th} data grid cell.
  - Short baselines (large-scale features) are weighted down.
  - Better resolution
  - Worse RMS noise
- Natural weighting: $W_k = 1/\sigma_k^2$, where σ_k^2 is the RMS noise
  - Short baselines are weighted up.
  - Best RMS noise across the image.
  - Effective resolution is less than 1/B.

Deconvolution/inversion methods

- Maximum Entropy Method
  - Tries to find an image that is consistent with data but has the maximum amount of entopy, i.e. smoothest image possible.
  - Does well with large scale diffuse emission, point sources are a problem.
- Variants of clean-algorithm:
  - Basic clean: scaled dirty beams are subtracted from the image plane until only residuals left. The positions and amplitudes are registered and these are replaced by a sum of Gaussians (clean-beams) with the same amplitudes.
  - Scale sensitive clean-variants: dirty beams are convolved with well-behaved functions (Gaussians, Hermitians etc.) with a number of sizes (scales) before clean-subtraction is done. The sum of the 'clean', unconvolved functions is the resulting image.
- Compressed sensing direct inversion
  - Based on a recently discovered algorithm utilizing **sparsity** of data in some domain and minimization of the L1-norm.
  - Prerequisites of convergence can be mathematically proved.